RICE UNIVERSITY

AN EXPERIMENTAL STUDY OF THE PRESSURE CONTOURS IN THE TURBULENT REATTACHMENT BUBBLE OF A BISTABLE FLUID AMPLIFIER

by

John Kirkpatrick

A THESIS SUBMITTED

IN PARTIAL FULFILLMENT OF THE

REQUIREMENTS FOR THE DEGREE OF

MASTER OF SCIENCE

Thesis Director's signature:

William F. Walker

Houston, Texas

January, 1968

ABSTRACT

AN EXPERIMENTAL STUDY OF THE PRESSURE CONTOURS IN THE TURBULENT REATTACHMENT BUBBLE OF A BISTABLE FLUID AMPLIFIER

by

John Kirkpatrick

An experimental study was conducted to determine the effect of aspect ratio, wall angle, and wall offset on the shape of pressure contours in the reattachment bubble of a symmetrical bistable fluid amplifier. The model was operated without control flow at a nominal nozzle exit Mach number of .45 and a nominal exit stagnation pressure of 4.05 "Hg. gauge exhausted to atmosphere. special attention was paid to trends in the location of and pressure within the minimum pressure region of the recirculation bubble. Pressure contour maps were graphed for aspect ratios of four, six, eight, and ten; offsets of two, four, and six nozzle widths; and wall angles of ten, twenty, and thirty degrees. The results are expressed as a series of pressure maps. The reattachment distances obtained were in fairly good agreement with the results found by others at lower Mach numbers.

Contents

NOMENCLATURE

α - angle receiver wall makes with centerline of model

C_p - specific heat (constant pressure)

δ - distance wall is offset from the edge of the nozzle

γ - ratio of specific heats C_p/C_v

h - nozzle height

k - thermal conductivity

i - number of primary variables used in dimensional analysis

K - number of primary dimensions used in dimensional analysis

M_e - exit Mach number

m - mass

NW - nozzle width(s)

ν - kinematic viscosity

P - local pressure in the flow field

P_a - atmospheric pressure

P_{min} - minimum local pressure measured in the flow field

P_s - nozzle exit static pressure

P_o - stagnation pressure measured upstream from the nozzle

ρ - density at the nozzle exit

π - dimensionless group

Q - a variable in an equation that is to be reduced by dimensional analysis

R - gas constant (for the gas in question)

T_e - nozzle exit temperature

θ - temperature

v_e - nozzle exit velocity

w - nozzle width

x - coordinate measured from the nozzle exit on a line parallel to the model centerline

y - coordinate measured from the model centerline on a line perpendicular to the centerline

I. INTRODUCTION

The phenomenon of a separated and reattached jet occurs in many phases of fluid dynamics. In particular, the device called a bistable fluid amplifier has become an object of much interest since its development in 1960. The effect depends on the fact that a jet of fluid which issues into a quiescent region of the same fluid will curve and attach to a wall which is within reasonable proximity. This is called the Coanda effect after the Rumanian engineer who rediscovered it. A bistable fluid amplifier has walls on either side of the jet. The jet may attach to either wall and with the addition of suitable switching controls to change the attachment from one wall to the other, forms a device which is applicable to fluid logic.

The basic qualitative description of the Coanda effect is fairly well known, but no one has yet published a study of the changes in pressure contours caused by changes in the geometric parameters of the amplifier: aspect ratio, the ratio of nozzle height to width; wall offset, the distance from the edge of the nozzle to the beginning of the sidewall, and wall angle, the angle between the sidewall and the nozzle centerline. Almost all the analytic work to date has been done on the problem of calculating the distance from the nozzle exit to the reattachment point. Almost always, a simplifying assumption has been made that the pressure in the recirculation bubble is constant. Although that assumption has been reported to be false in several sources and thus does not require any further refutation, it is hoped that a systematic analysis of pressures will shed additional light on the pressure distributions and enable analysts to construct more accurate models.

McCoy's work[7] contains a list of many available references in the field of fluidics published before the summer or 1967. Kirshner's book[6] is a summary of the state of the art up to early 1966. NASA report CR-101[4] is a bibliography of references from before the fall of 1964. A very recent paper by Jones et al[5] presented some numerical study on the problem of the distribution of pressures at the wall.

All the available analytic work in subsonic flow assumes incompressibility. The data presented here was taken at a Mach number of about .45 which is within the range of numbers for which compressibility effects may be somewhat important. Apparently all analyses leave at least one empirical parameter to absorb errors, usually the spread parameter which is defined in a manner analogous to that in a free jet. In Bourque's latest paper[1], he chose a value of the parameter which he thought gave the best fit to experimental results. He is the only researcher whose work has yet come to light who has felt confident enough to predict reattachment distance given only wall angle and offset.

The remaining sections of this thesis will deal with a dimensional analysis, a description of the model and its instrumentation together with the design criteria involved in their construction, the experimental procedure used, and a qualitative discussion of the experimental results. The last pages contain pictures of the apparatus and then a set of experimental pressure maps for different geometries.

II. DIMENSIONAL ANALYSIS

A dimensional analysis can be helpful in delineating the non-dimensional variables which may influence a phenomenon. There is quite a bit of latitude available in current methods and thus the analysis may give several different possible results. This latitude means that an analyst may be able to pick a set of dimensionless groups which are particularly convenient to measure with his equipment or apply to the data he has at hand.

The first step is to select the dimensioned variables that are likely to affect the phenomenon. Obviously this choice requires some judgements. These variables must be analyzed and their "primary dimensions" identified. The choice of primary dimensions is somewhat arbitrary, the only constraint being that the set must include all the dimensions of the variables which have been selected as important to the study.

The Buckingham Pi Theorem states that if a physical equation exists between n variables, it may equivalently be expressed as an equation between n-K dimensionless groupings of these variables where K is less than or equal to the number of primary dimensions involved in the n variables(3). If Q is used to denote a physical variable and π a dimensionless combination of Q's, the theorem states that a functional relation of the form

$$f(Q_1 \ldots\ldots Q_n) = 0$$

can be expressed as a function of dimensionless groups of the form

$$\phi(\pi_1 \ldots\ldots \pi_{n-K}) = 0 \qquad K \leq i$$

The number of independent dimensions is denoted by i. Each π is of the form

$$\pi = Q_1{}^a Q_2{}^b \ldots\ldots Q_n$$

where the exponents are adjusted to leave π with no dimensions.

Using the method explained by Chapman(3), the Pi theorem can be used to systematically combine the n variables into n-i dimensionless groups. After the dimensioned variables and primary dimensions have been chosen, i of the variables must be selected for use as "primary variables". This choice is free provided that the set of primary variables contains all the primary dimensions among its members, that they do not form a dimensionless product themselves, and that no two of them have identical dimensional configurations.

The primary dimensions selected for this analysis were length L, time t, temperature Θ, and mass m. The significant variables and their dimensions are

local pressure	P	(m/Lt^2)
wall angle (radians)	α	(1)
nozzle width	w	(L)
nozzle height	h	(L)
wall offset	δ	(L)
nozzle exit temperature	T_e	(Θ)
nozzle exit static pressure	P_s	(m/Lt^2)
nozzle exit velocity	v_e	(L/t)
nozzle exit density	ρ	(m/L^3)
kinematic viscosity	ν	(L^2/t)
specific heat (constant pressure)	C_p	$(L^2/\Theta t^2)$
thermal conductivity	k	$(mL/\Theta t^3)$
stagnation pressure	P_o	(m/Lt^2)

distance from nozzle exit x (L)

distance from nozzle centerline y (L)

The set of primary variables which gave the most useful results were P_o, w, ρ, and C_p. Using the method outlined in Chapman, the following functional form was found:

$$\frac{P}{P_o} = f\left(\frac{x}{w}, \frac{y}{w}, \frac{h}{w}, \frac{\delta}{w}, \alpha, \frac{P_s}{P_o}, \frac{\rho C_p T_e}{P_o}, \frac{k^2}{\rho P_o w^2 C_p^2}, \frac{\rho V_e^2}{P_o}, \frac{\rho \nu^2}{P_o w^2}\right)$$

It is permissible to multiply the non-dimensional groups together. This process can result in a lessening of the number of groups or a more convenient set. If the working fluid is assumed a perfect gas, then $\frac{\rho C_p T_e}{P_o}$ becomes $\frac{P_s C_p}{P_o R}$ which is C_p/R multiplied by P_s/P_o, a group which is already in the functional.

$$\frac{k^2}{\rho P_o w^2 C_p^2} \frac{P_o w^2}{\rho \nu^2} = \frac{k^2}{C_p^2 \mu^2}$$

This gives the Prandtl number squared.

$$\frac{\rho V_e^2}{P_o} \frac{P_o w^2}{\rho \nu^2} = \frac{V^2 w^2}{\nu^2}$$

This gives the Reynolds number squared. So the final form becomes

$$\frac{P}{P_o} = f\left(\frac{x}{w}, \frac{y}{w}, \frac{h}{w}, \frac{\delta}{w}, \alpha, \frac{P_s}{P_o}, \frac{V_e w}{\nu}, \frac{C_p}{R}, \frac{k}{C_p \mu}\right)$$

In the work done for this thesis, the last two groups were held constant by always using air at an approximately constant temperature. P_s/P_o was held approximately constant and all the remaining groups were varied. Unfortunately there was no way to hold Reynolds number constant and vary the aspect ratio (h/w) without also varying P_o. Thus the effects of aspect ratio and Reynolds number were combined. There is some evidence that Reynolds number may not have had any significant effect on this experiment. Bourque and Newman(2) found that reattachment distance and flow rate were essentially independent of Reynolds number for values above about 5,500. Their data was taken at a pressure ratio of P_o/P_s less than 1.1 which means a Mach number less than .27, well within the incompressible range. McRee and Moses[8] presented data relating reattachment length to Reynolds number and found that the effect was quite significant in the range from 2,000 to 8,000. But the effect was much less pronounced above 6,000. For their data the incompressibility assumption was "consistent with the range of experiment". Though the point was not made entirely clear, they seem to have varied Reynolds number by varying aspect ratio so that the effects were combined. The data taken for this work was at a Mach number of .45 and Reynolds numbers ranging from 60,000 to 118,000. Though the point is no doubt open to some further debate, it will be assumed that the data presented her is independent of Reynolds number. This assumption is justified because the Mach number was not high enough for compressibility effects to be judged predominant while at the same time the Reynolds numbers were ten times higher than that value at which other experimenters have found Reynolds number dependency to vanish in incompressible flow.

III. APPARATUS AND INSTRUMENTATION

The model used in this experiment was designed by McCoy(7). It is illustrated in figures 2 through 8. The model was designed to permit great flexibility in the adjustment of wall angle, offset, and aspect ratio. It was sized large enough to permit the use of the instruments hopefully without too much disturbance of the flow field. The air supply was a Schramm reciprocating compressore rated at 200 scfm at 100 psig. This high flow rate enabled use of a large model with a wide range of subsonic Mach numbers.

The final height was two inches plus gasketting. The nozzle blocks were machined from two-inch thick pieces of aluminum and shaped to allow the flow to stagnate and then accelerate smoothly to the exit. The stagnation chamber measured from sixteen to forty times the area of the exit slot in the tests cited here. A static pressure tap was drilled in the side of one block near the exit and a stagnation pressure probe was mounted in the center of the stagnation chamber. At first the flow had a tendency to attach to one wall of the wedge-shaped inlet diffuser as it left the supply pipe, but this was corrected by placing some wire screen over the mouth of the diffuser. Oblong holes were drilled in the nozzle blocks and diffuser backing plate so the blocks could be moved to vary aspect ratio.

The side walls were made from two-inch square aluminum tubing twenty-six inches long. This length was twice or more any measured reattachment distance, which assured that the length of the wall would not affect the reattachment distance(2). The top plate was made of 3/16" aluminum plate and the bottom of 1/8" steel. The top and bottom of the side walls and nozzle blocks, the outer face of the nozzle blocks, and the diffuser backing plate were covered with soft rubber gaskets an eighth of an inch thick. The blocks and walls were held in place by the pressure from the top and bottom plates which were squeezed together by a series of bolts running through them. The diffuser was held in place by bolts attached to the top, bottom, and nozzle blocks.

One of the instruments used was a 30", United Sensor Corporation, three-dimensional pressure probe (figure 5). This was rigidly attached to a steel block with a threaded hole in it (see figure 3). A long piece of threaded rod led through this hole and was held in place in bearings at either end. As the rod turned, the block and probe were traversed in a direction perpendicular to the centerline of the model. The rod bearings were mounted on a rack which was moved back and forth by a gear, which accomplished motion parallel to the centerline. Both degrees of freedom were measured with scales divided into hundredths of an inch.

The three-dimensional probe was useless for flows which diverged more than thirty degrees from the centerline of the model. The only instrument at hand which seemed to give promise of being useful for all flow directions was a wedge-head, two-dimensional United Sensor probe inserted through holes in the top (figure 4). A grid of holes was drilled in the top plate with centers spaced half an inch apart so that the probe could be lowered into any part of one side of the centerline which might be of interest. Each hole was covered with a patch of duct sealing tape. A stand was built for the probe and a protractor was mounted to measure the flow direction. The stand was adjusted so that the pressure taps in the probe were halfway between the top and bottom plates.

The stagnation temperature was measured at a thermowell inserted into the diffuser at a slant. The sensing element was a mercury type connected to a remote dial. All pressures were measured on U-tube manometers. Atmospheric pressured was measured with an Army Signal Corps type mercury barometer.

The air supply was carried from the compressor to a large receiver tank. From there it was piped to a one-inch Watts high capacity pressure regulator. The regulator was linked to the diffuser inlet by a length of high-pressure rubber hose to dampen vibrations.

IV. EXPERIMENTAL PROCEDURE

The first step in preparing for a data run was setting the geometry. Four accurately machined metal blocks mounted on rods were provided to set nozzle width. The nozzle blocks were adjusted to this width and then the offset and wall angle were set with a scale and protractor. The top plate was carefully lowered into place and bolted down and then the nozzle width measuring block was removed.

One data run was made for each combination of aspect ratio, wall angle, and offset. But the aspect ratio of ten and offset of two nozzle widths settings were so small that there could be but two points in the traverse at the widest part. This was deemed too small an amount of information to make a pressure map. The apparatus required up to half an hour to attain equilibrium temperature. When the equilibrium was reached, the values of atmospheric pressure P_a, stagnation pressure P_o, exit static pressure P_s, and stagnation temperature T_o were recorded. The next step was to measure the reattachment length, for which the three-dimensional probe proved useful. Some tests made by moving the three-dimensional probe away from the nozzle with its tip always against the wall had shown that the impact pressure and one of the static pressures were almost the same for much of the distance in the recirculation bubble. The impact pressure was usually a little less than the static while the probe was still within the bubble. But at a certain point the impact pressure began to be larger than the static and the pressures diverged as the probe moved farther away (see figure 6). It was reasoned that the point where the pressures were the same was probably a stagnation point and thus corresponded to the reattachment point. In the normal runs, the point was found by observing a water manometer set to read P_1-P_4 (refer to figure 5 for locations of pressure taps). The air flow left a fine oil deposit on the top and bottom plates and the wall to which it was attached (figures 7b and 8c). These marks made it possible to define the reattachment point within limits. The point at which the pressures in the three-dimensional probe began to diverge always fell within these limits. Throughout the experiments, the reattachment length as determined by the probe was checked against the oil streaks whenever possible.

After the reattachment length was determined, readings were taken with the wedge-head probe at all stations for which holes were drilled. This meant that readings covered the region bounded by the face of the nozzle block, the side wall, the centerline of the model, and the line of holes immediately downstream from the reattachment point. The wedge head probe has three pressure taps (see figure 4): P_1 the impact pressure, and P_2 and P_3 the static pressures on either face of the wedge. The information recorded at each point was $P_1-\frac{1}{2}(P_2+P_3)$, $\frac{1}{2}(P_2+P_3)-P_a$, and flow direction. When the axis of the wedge is pointed in the direction of the flow, P_2 and P_3 are equal. A water manometer was included in the instrumentation which indicated P_2-P_3. When this read zero, the probe was aligned with the flow and the flow direction was read from the protractor. Since the pressures could be balanced at either of two directions 180 degrees apart, the direction which produced the larger value of impact minus average static pressure $(P_1-\frac{1}{2}(P_2+P_3))$ was judged the correct flow direction.

There are several possible sources of error in the experimental technique. The values of P_o, P_s, P_a, and T_o were not always the same from one run to the next. In addition there was usually some slow drift during the longer test runs, some of which took as long as ten hours. But the total errors were all less than one percent of the absolute values of the variables involved. The P_o, P_s, P_a, and T_o cited in this work are often averages of readings taken at intervals during the particular runs. Rechecks of reattachment length showed that this distance was unaffected by such drifts as occurred. The values of exit Mach number M_e were calculated from the averages assuming air a perfect gas with $\gamma=1.4$ and

$$\frac{P_o}{P_s} = \left(1 + \frac{\gamma-1}{2} M_e^2\right)^{\frac{\gamma}{\gamma-1}}$$

Repeatability tests were taken on selected points with P_o deliberately varied from 3.8 to 4.2" Hg. gauge which showed possible variations of up to .9" H_2O in the static pressures.

The static pressure maps how the isobars in the flow field. The x and y coordinates are shown normalized with respect to nozzle width. The isobars respresent gauge pressure in "H_2O as read by a water manometer vented to the atmosphere. While the dimensional analysis indicated that the representation should show non-dimensional pressure P/P_o rather than $P-P_a$, there are several other possible coefficients that could conceivably be used. Examples are $(P-P_a)/(P_o-P_a)$, $(P-P_a)/\frac{1}{2}\ v_e^2$, and $Pw^2/\rho\nu^2$. The latter arose from taking a dimensional analysis using ρ, w, ν, and C_p as the primary variables. It was felt best to leave the pressures in the raw state and let those who wish to use the data relabel the isobars to suit whichever coefficient they feel is applicable in their work.

The obvious features appearing in the pressure maps are the reattachment point and the minimum pressure region of the recirculation bubble. Reattachment length was compared against other extant data. The papers by Olson and his associates[9] reported that wall pressure distribution may be generalized in terms of percentage distance to reattachment. But Jones et al[5] apparently didn't find this to be so. The maps in this thesis could not be used to check this observation because the intersection of a given isobar with the wall depends largely on the whim of the draftsman. However, it was decided to see if the minimum pressure region occurred at the same percentage of reattachment. For this purpose, two ratios were created. The first took the approximate x-coordinate of the minimum pressure center and divided it by the x-coordinate of the reattachment point (such ratio designated x_{pc}/x_{att}). The second, designated y_{pc}/y_w, took the approximate y-coordinate of the pressure center and divided it by the distance from the centerline to that wall as measured along a line through the low pressure center perpendicular to the centerline. These two geometric ratios and the minimum measured value of pressure (P_{min}) were checked for trends in their values as the geometric parameters of the amplifier varied. Where trends occurred, the quantities were plotted against the geometric parameter being varied, but no acceptable correlations were found from plots on square, semi-log, and log-log paper. In some cases, notably when the results from different aspect ratios were being compared, one or more of the geometric ratios should have stayed almost constant since the numerator and denominator were fairly close, but apparently the errors inherent in estimating x_{pc}, y_{pc}, y_w, and x_{att} combined to produce too much scatter to make a quantitative worthwhile.

V. EXPERIMENTAL RESULTS

Effects of Change of Aspect Ratio

Comparison of the pressure maps for different aspect ratios was especially important since this would tell whether or not there was much similarity in the flows when wall angle and offset were held constant. The ratios x_{pc}/x_{att} and y_{pc}/y_w were scattered. They showed no apparent trends and rarely showed a spread of less than twenty percent. P_{min} usually went down (i.e. became more negative) with increasing aspect ratio. The actual x- and y-coordinates of the low-pressure center as expressed in nozzle widths behaved much better than the ratios. The pressure center locations were generally within ten percent of an average value for each set of angles and offsets. The reattachment distance also stayed within ten percent for a given combination of offset and wall angle. The averages were also close to Bourque's latest predictions(1). Apparently, the effect of compressibility on the reattachment length was not very significant at a Mach number of .45. There is a group of isobars near the nozzle which are almost parallel to the centerline. As aspect ratio increased, these isobars seemed to become more squeezed together so that the apparent pressure gradient in a direction perpendicular to the centerline increased in that region.

Effects of Change of Offset

Qualitatively the effects of offset variation were as expected. As offset lessened, the reattachment length, x- and y-coordinates of the minimum pressure center, and overall size of the recirculation region all shrank. In almost all cases P_{min} went down as offset and therefore the area available for aspiration decreased. No provable trend was shown by x_{pc}/x_{att}. But as offset decreased, y_{pc}/y_w went up. This means that as the wall moved closer to the centerline, the distance from the wall to the minimum pressure center as a percentage of the distance from the wall to the centerline at the same x-distance became less. Thus the wall moved closer to the centerline relatively speaking than did the pressure center. The isobars near the nozzle parallel to the centerline moved closer together as the offset increased.

Effects of Change of Wall Angle

Wall angle also produced about the expected results. As wall angle decreased, reattachment length, x- and y-coordinates of the minimum pressure center, and the overall size of the recirculation region shrank. By looking at the patterns, one can conclude that the isobars around the low pressure center often were approximately circular at thirty degrees, but as the wall angle decreased they became more oval. As wall angle lessened, x_{pc}/x_{att} also dropped. P_{min} and y_{pc}/y_w showed no apparent trends. The isobars near the nozzle were squeezed together only slightly compared to the more noticeable squeezing accompanying aspect ratio and offset changes.

General Comments

The accuracy of the drafting method did not allow a check on Olson's contention that pressures along the wall could be generalized in terms of percentage of distance to reattachment. Some cursory attempts to gain a wall pressure profile with the three-dimensional probe seemed to cast considerable doubt on Olson's findings. Olson's measurements were taken with pressure taps set in the wall and thus measured pressure in the boundary layer. The measurements just mentioned were taken from the P_4 tap of the three-dimensional probe, which meant that the tap could never be closer than about .07" from the wall. These measurements were therefore taken outside or near the edge of the boundary layer. The location of the low-pressure center did not even approximately have the same x_{pc}/x_{att} values. Measured values of this quotient ranged from .4 to .8. If Olson is correct in saying that the wall pressure profile is a function of percentage distance to reattachment, then the wall pressures must be almost independent of the nature of the interior pressures.

Care should be taken not to invest the graphs presented here with the attributes of gospel. They were drawn by linear interpolation from a finite grid of points which in the cases of the smaller-sized models (i.e. those with a high aspect ratio and low offset and wall angle) was quite coarse. In addition, there was some drift in the control pressures and temperature as already mentioned. The presence of the pressure probe influenced the pressures to an unknown degree which might have been quite severe in the small sizes. The maps thus only show approximate contours which give only the general outline of the pressure field and not its exact shape.

VI. BIBLIOGRAPHY

1. Bourque, C., "Reattachment of a Two-Dimensional Jet to an Adjacent Flat Plate," Advances in Fluidics, American Society of Mechanical Engineers, New York, 1967

2. Bourque, C., and B.G. Newman, "Reattachment of a Two-Dimensional Incompressible Jet to an Adjacent Flat Plate." The Aeronautical Quarterly, XI, August, 1960.

3. Chapman, A.J., Heat Transfer, 2nd edition, Macmillan, New York, 1967.

4. Fluid Amplifier State of the Art Vol. I, Research and Development--Fluid Amplifiers and Logic," NASA Contractor Report CR-101, NASA, Washington, D.C., 1964.

5. Jones, N.S., K. Foster, and D.G. Mitchell, "A Method of Calculating the Wall Pressure Distribution in a Turbulent Reattachment Bubble," Second Cranfield Fluidics Conference, Cambridge, England, January, 1967.

6. Kirshner, Joseph M., Fluid Amplifiers, McGraw-Hill, New York, 1966.

7. McCoy, J.J., Jr., "An Experimental Study of the Effect of Aspect Ratio, Wall Angle, and Wall Offset on the Resultant Force on the Two-Dimensional Jet in Bistable Fluid Amplifiers," Thesis submitted at Rice University, September, 1967.

8. McRee. D.I., and H.L. Moses, "The Effect of Aspect Ratio and Offset on Nozzle Flow and Jet Reattachment", Advances in Fluidics, American Society of Mechanical Engineers, New York, 1967.

9. Olson, R.E., and R.C. Stoeffler, "Analytical Method for Predicting Power Jet Reattachment Characteristics in Wall-Attachment-Type Fluidic Devices", Advances in Fluidics, American Society of Mechanical Engineers, New York, 1967.

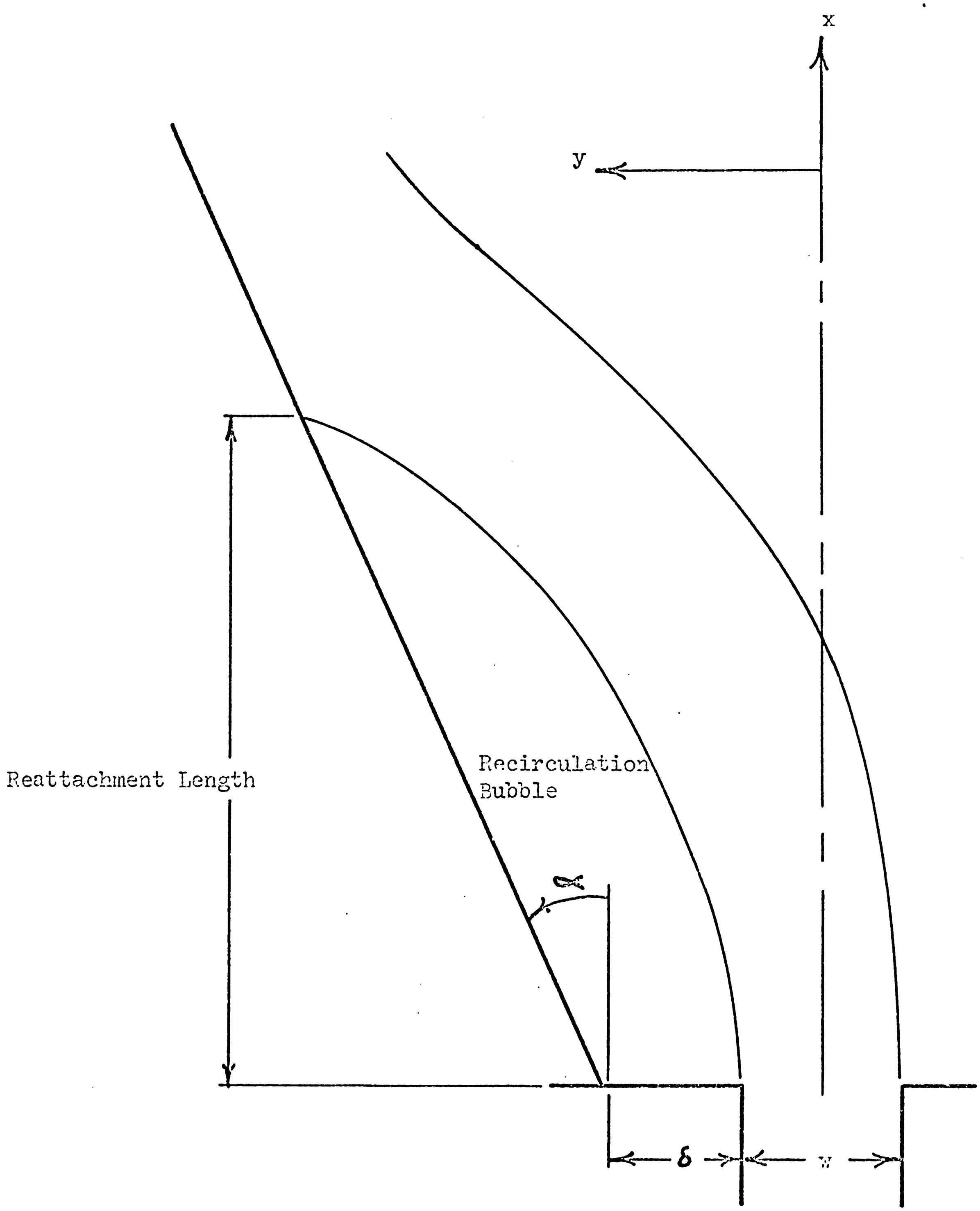

Fig. 1 Diagram of Fluid Bistable Element

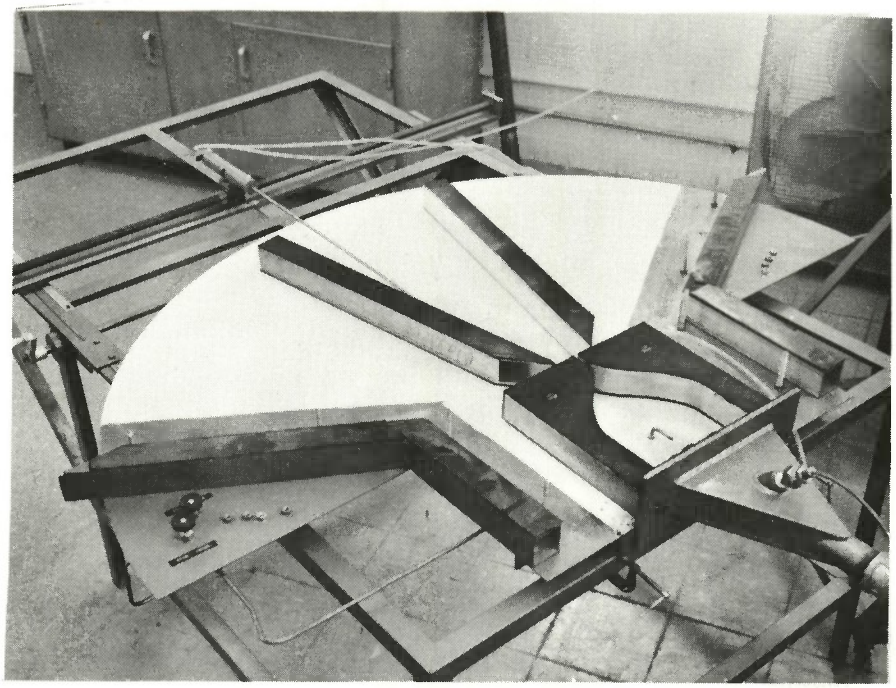

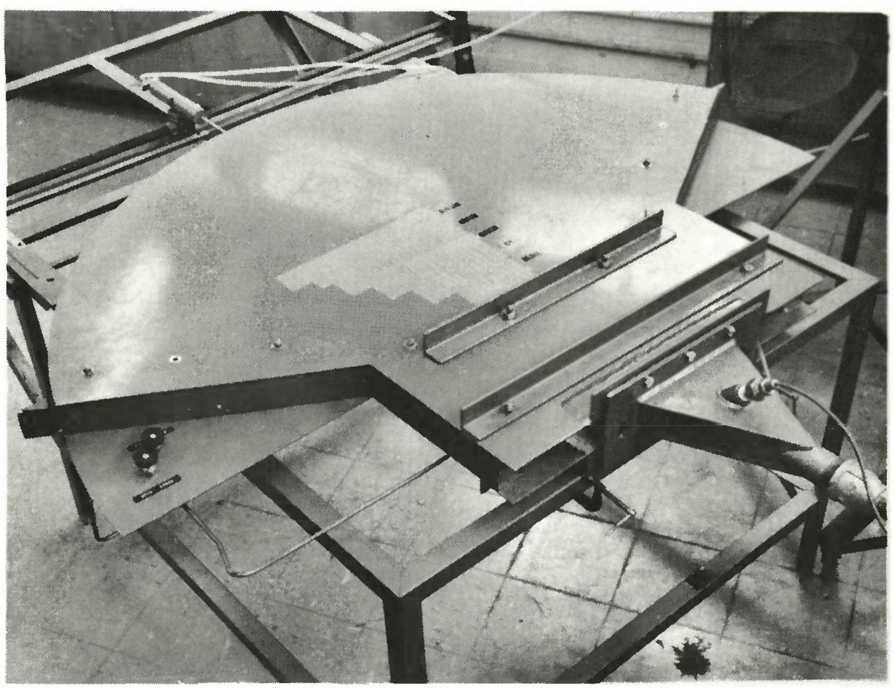

Figure 2a, top: Model Fluid Amplifier with top removed

Figure 2b, bottom: Model with top clamped on.

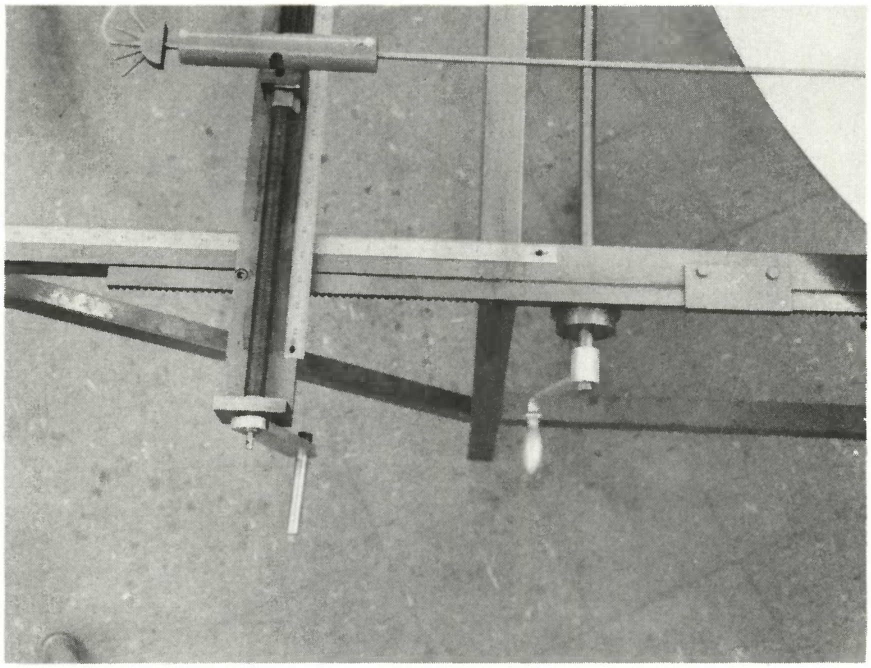

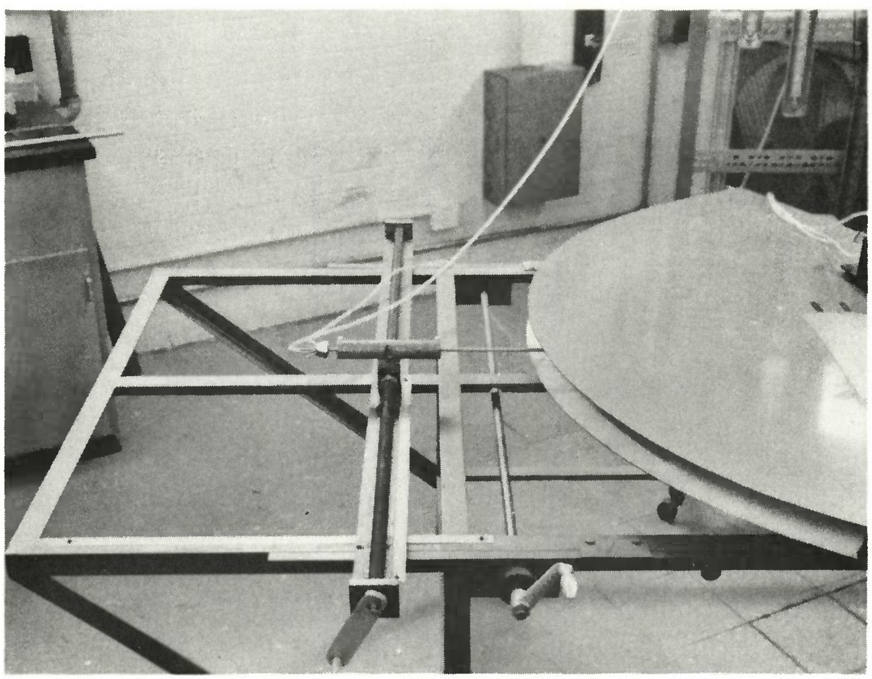

Figure 3a, top: Closeup of probe positioner

Figure 3b, bottom: Probe positioner mounted on table

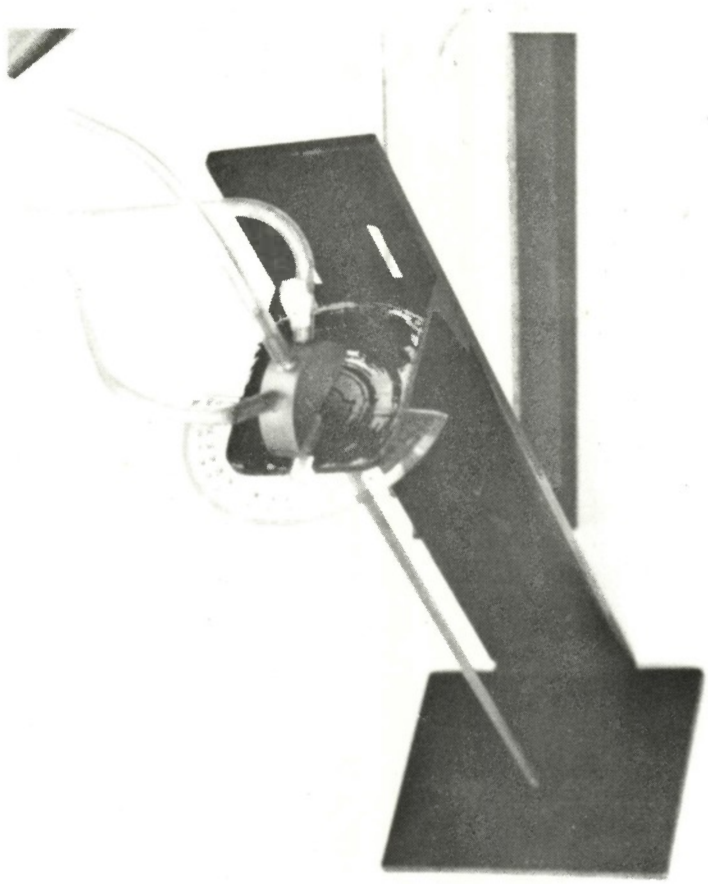

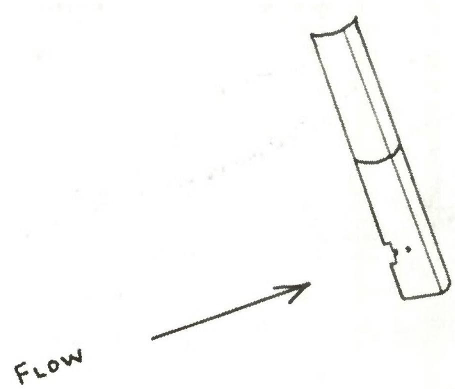

Figure 4a, top: Two-Dimensional Probe and mount

Figure 4b, bottom: Sketch showing position of pressure taps

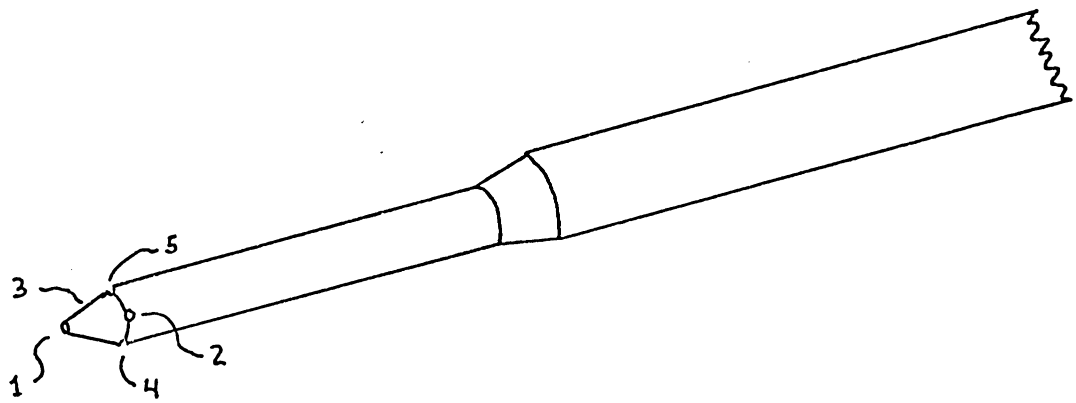

Figure 5: Three-Dimensional Probe used to locate attachment point

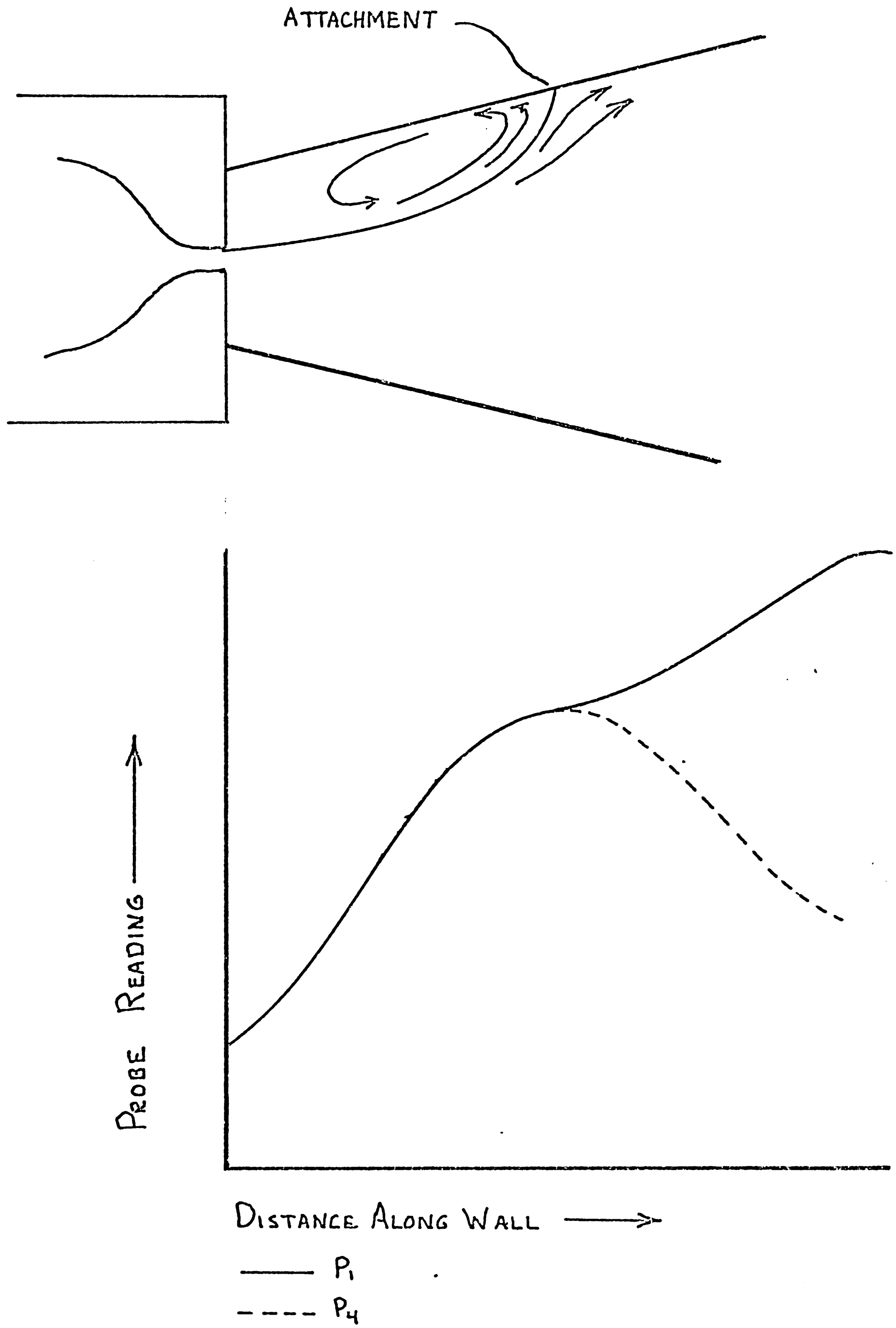

Figure 6: Qualitative picture of static pressure along wall

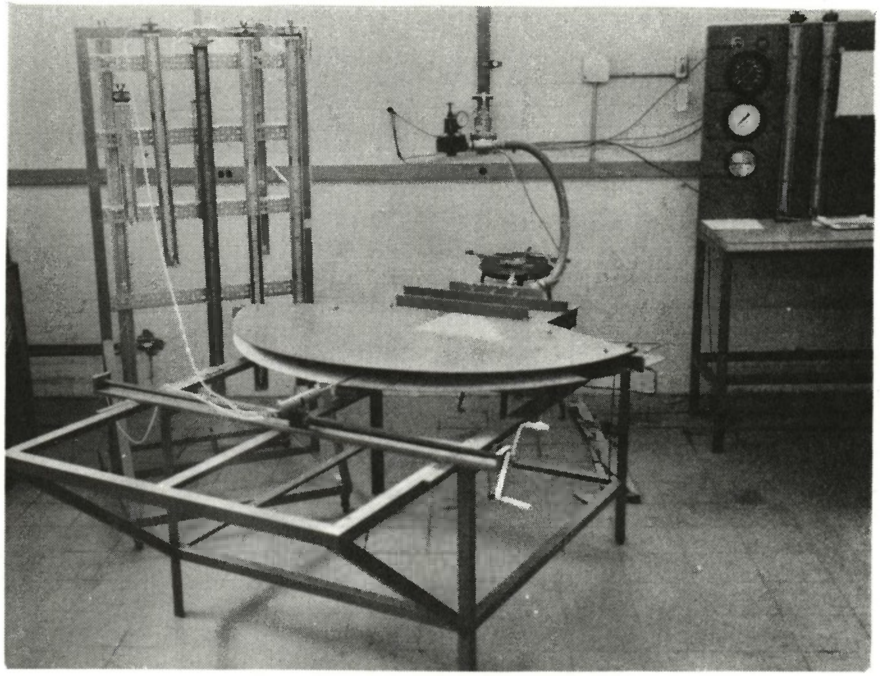

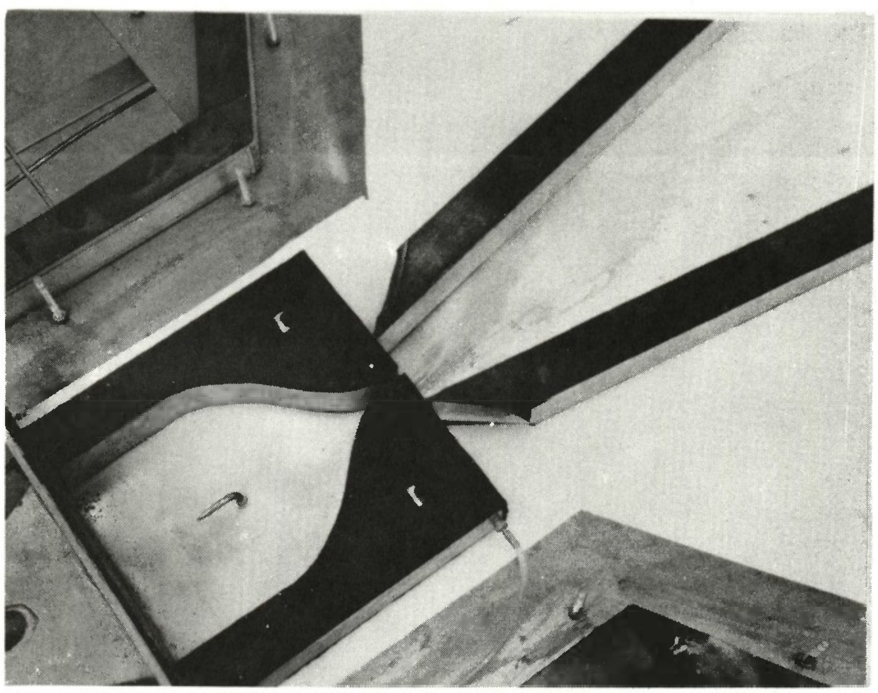

Figure 7a, top: Model on table, with Manometer rack beside

Figure 7b, bottom: Top view showing oil streaks

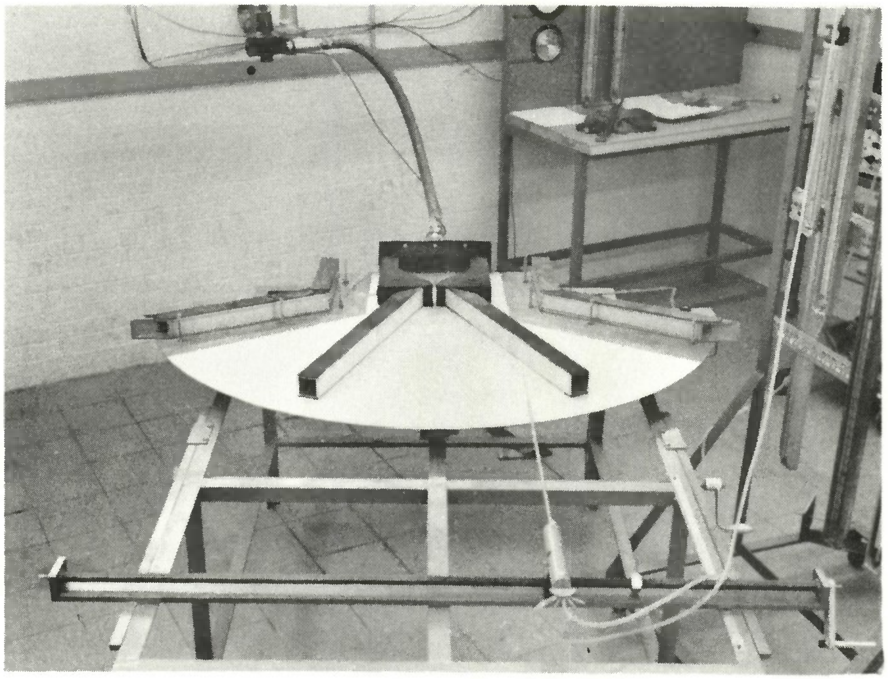

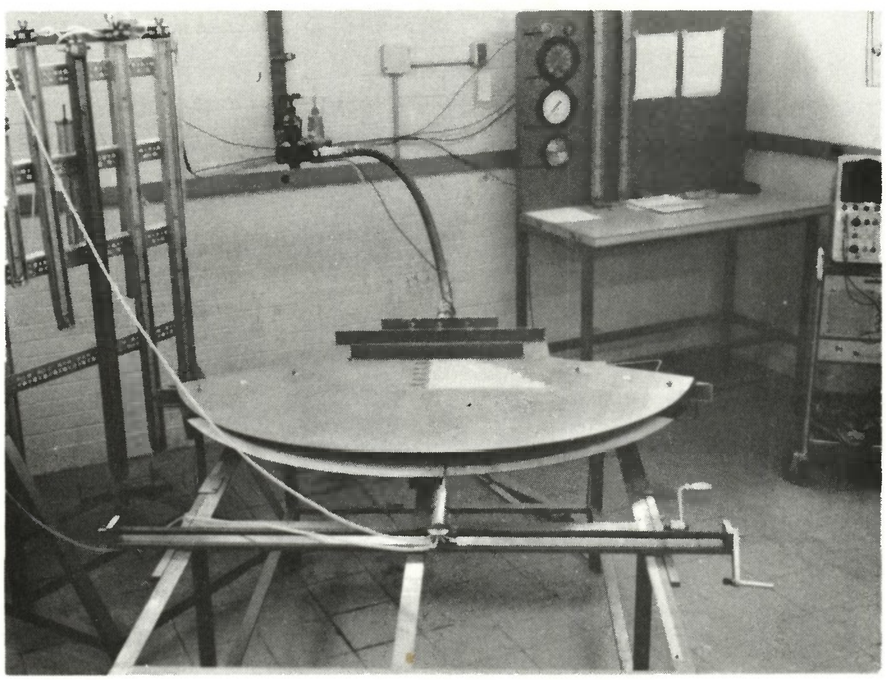

Figure 8a, top: Front view of apparatus with top off

Figure 8b, bottom: Front view with top on

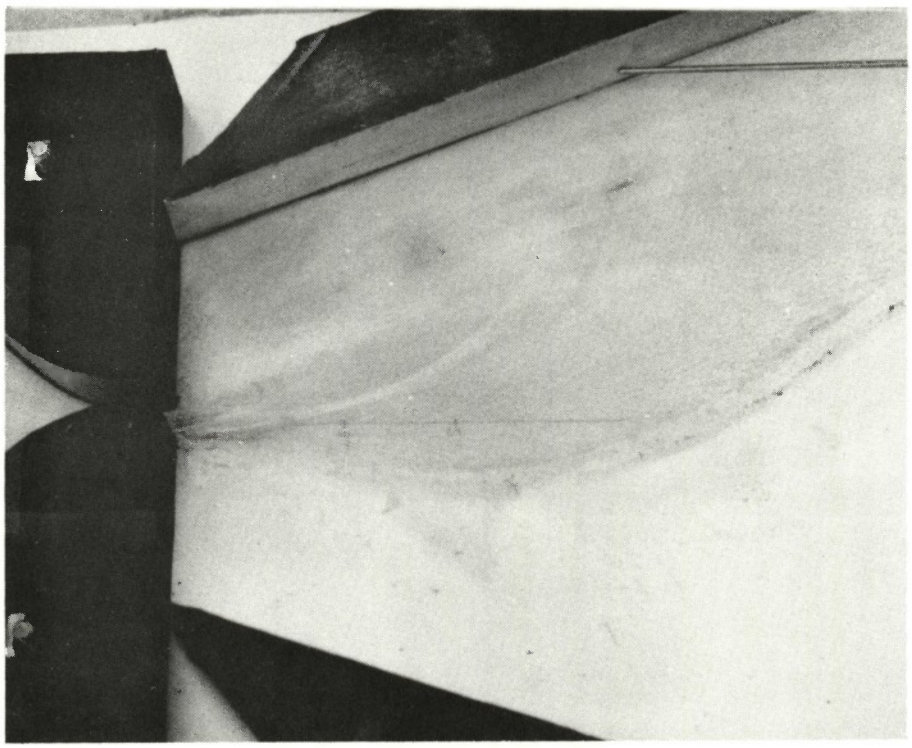

Figure 8c: Top view showing oil streaks

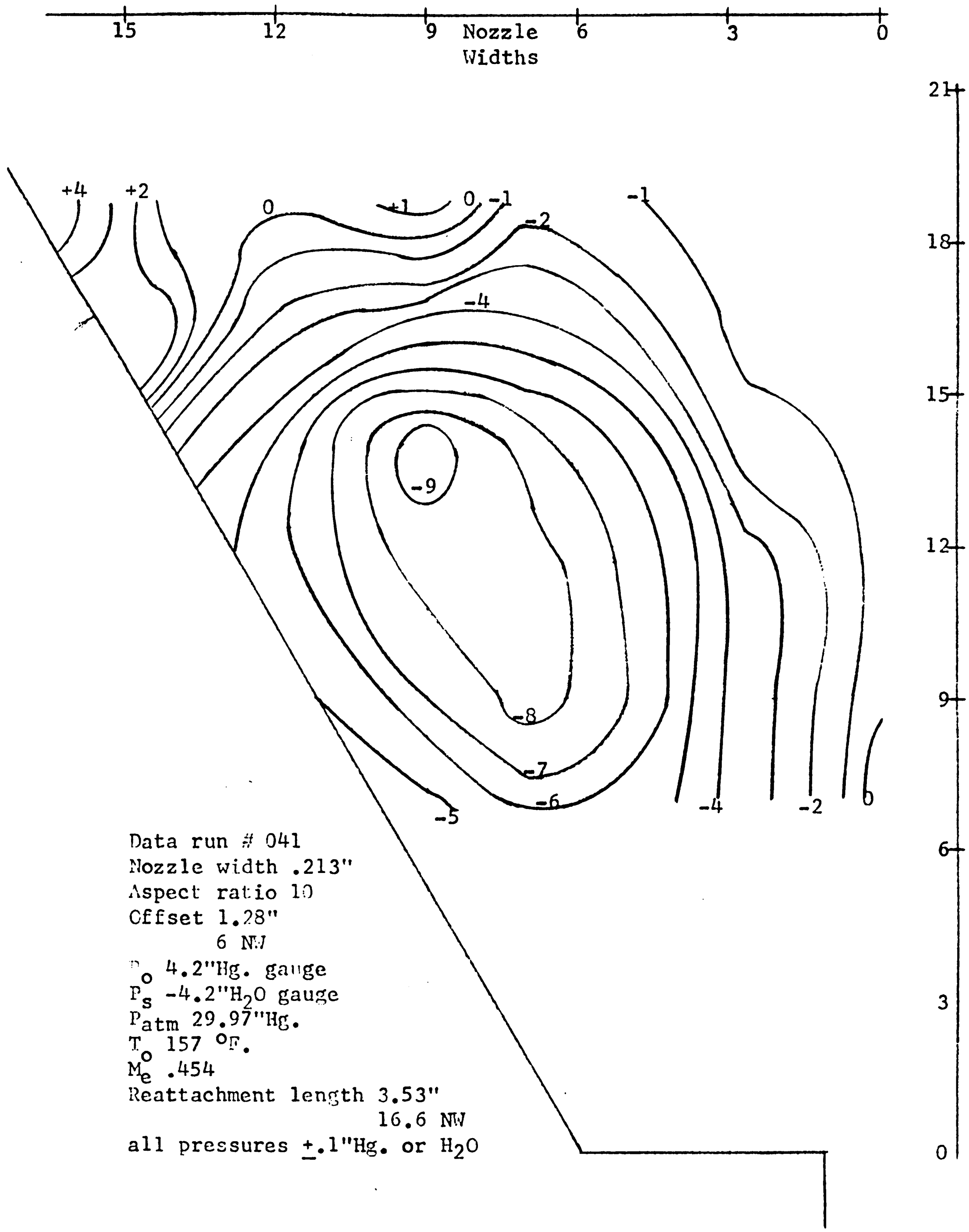

Data run # 041
Nozzle width .213"
Aspect ratio 10
Offset 1.28"
6 NW
P_o 4.2"Hg. gauge
P_s -4.2"H_2O gauge
P_{atm} 29.97"Hg.
T_o 157 ^oF.
M_e .454
Reattachment length 3.53"
16.6 NW
all pressures ±.1"Hg. or H_2O

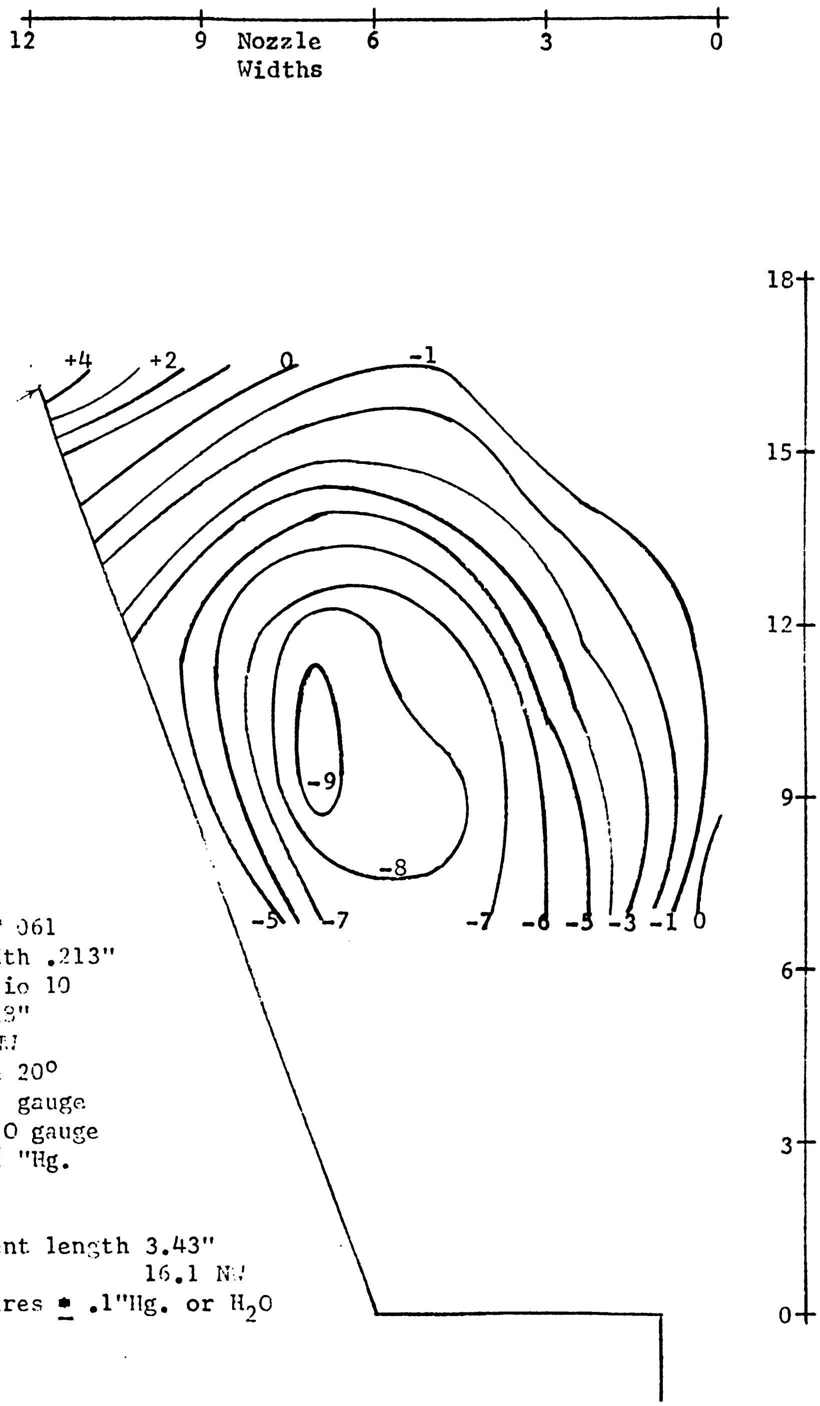

Data run # 061
Nozzle width .213"
Aspect ratio 10
Offset 1.28"
6 NW
Wall angle 20°
P_o 4.0"Hg. gauge
P_s -4.0"H_2O gauge
P_{atm} 29.92 "Hg.
T_o 158°F.
M_e .444
Reattachment length 3.43"
16.1 NW
all pressures ± .1"Hg. or H_2O

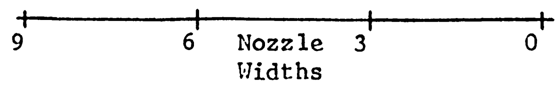

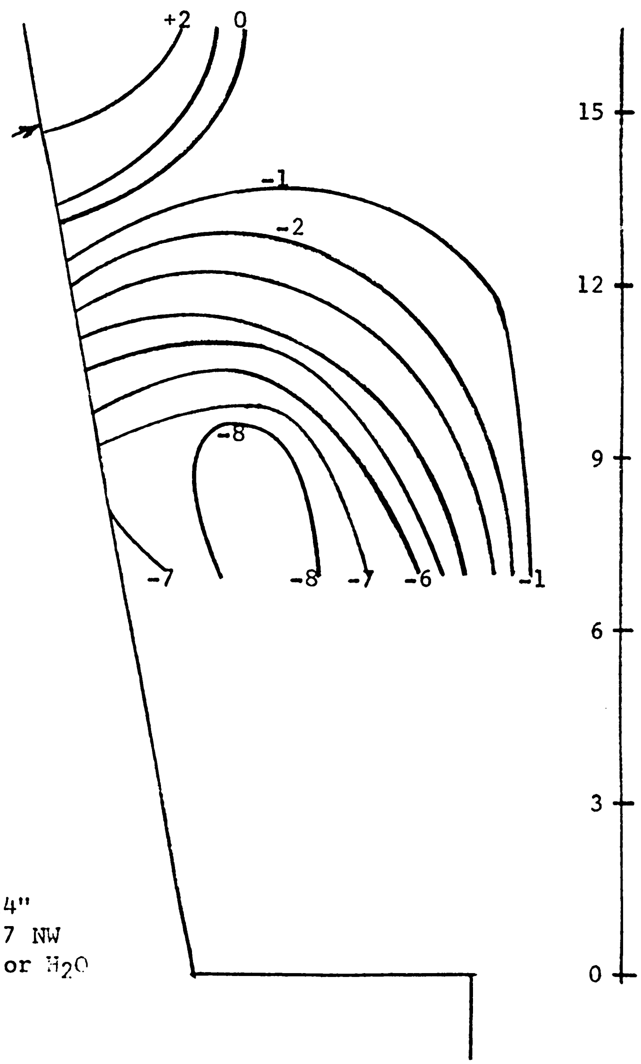

Data run # 062
Nozzle width .213"
Aspect ratio 10
Offset 1.28"
6 NW
Wall angle 10^{o}
P_o 4.0"Hg. gauge
P_s -5.1"H_2O gauge
P_{atm} 29.92"Hg.
T_o 150^{o}F.
M_e .449
Reattachment length 3.14"
14.7 NW
all pressures ± .1"Hg. or H_2O

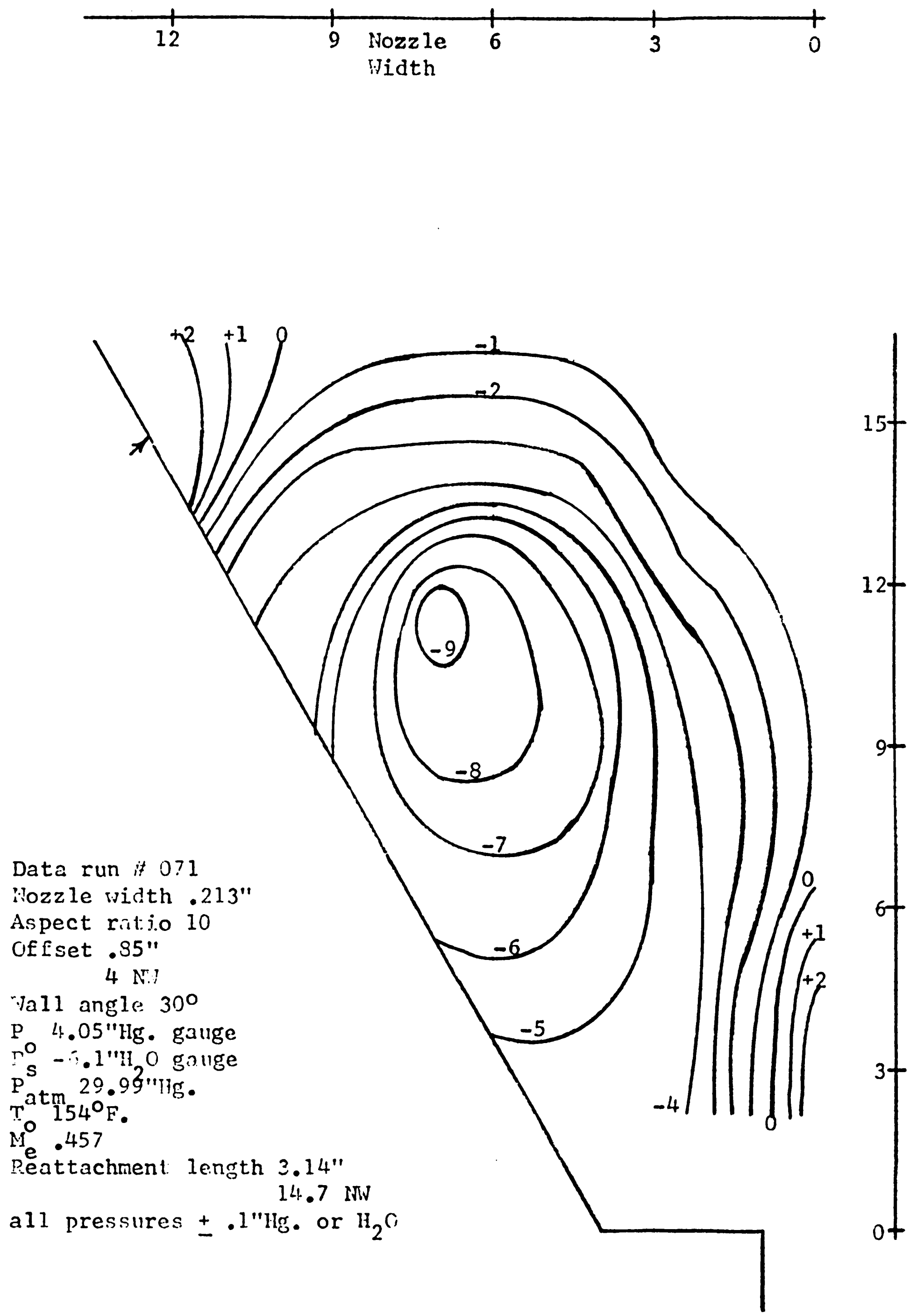

12
9
Nozzle Width
6
3
0
+2
+1
0
-1
-2
-9
-8
-7
-6
-5
-4
0
+1
+2
0
15
12
9
6
3
0
Data run # 071
Nozzle width .213"
Aspect ratio 10
Offset .85"
4 NW
Wall angle 30°
P_o 4.05"Hg. gauge
P_s -6.1"H_2O gauge
P_{atm} 29.99"Hg.
T_o 154°F.
M_e .457
Reattachment length 3.14"
14.7 NW
all pressures ± .1"Hg. or H_2O

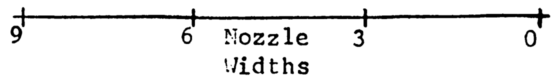

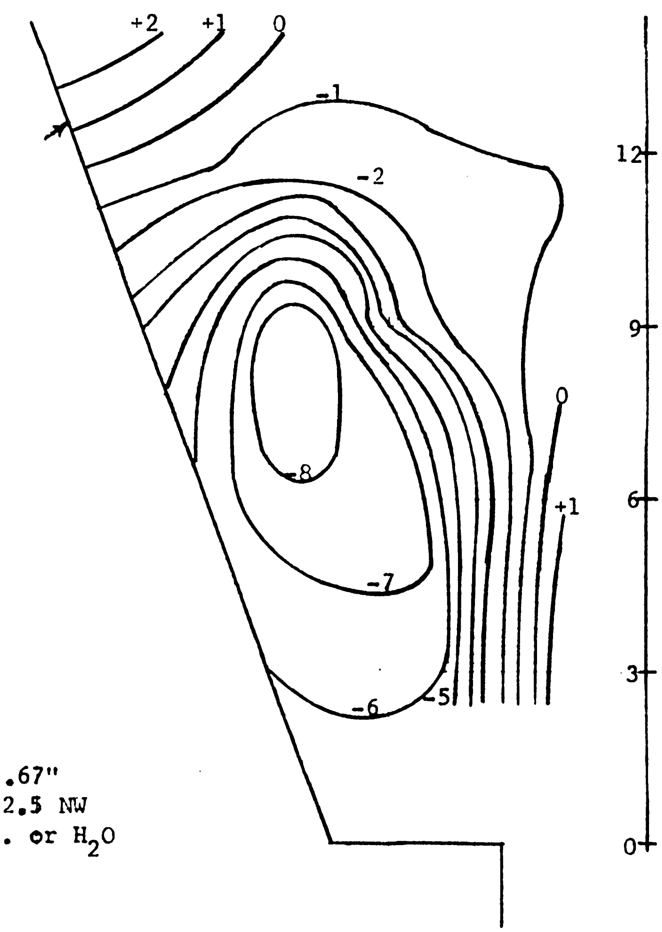

Data run # 072
Nozzle width .213"
Aspect ratio 10
Offset .85"
4 NW
Wall angle 20°
P_o 4.0"Hg. gauge
P_s -6.4"H_2O gauge
P_{atm} 29.95"Hg.
T_o 161°F.
M_e .455
Reattachment Length 2.67"
12.5 NW
all pressures ± .1"Hg. or H_2O

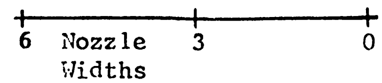

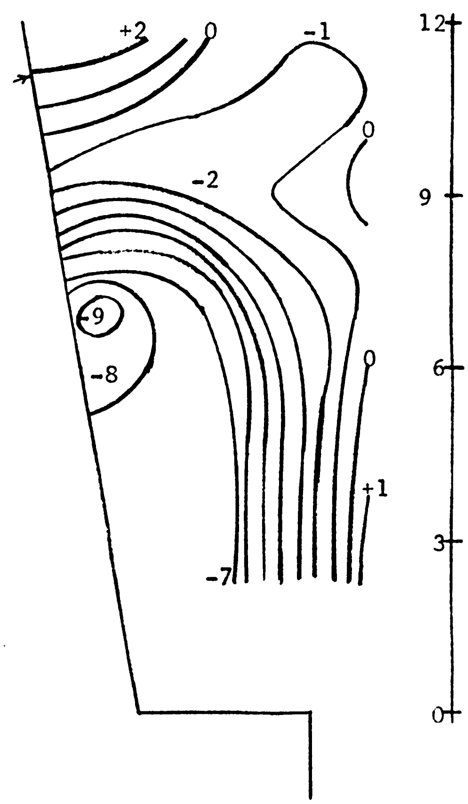

Data run # 073
Nozzle width .213"
Aspect ratio 10
Offset .85"
4 NW
Wall angle 10^{o}
P_o 4.05"Hg. gauge
P_s -6.4"H_2O gauge
P_{atm} 29.94"Hg.
T_o 158^{o}F.
M_e .456
Reattachment length 2.36"
11.1 NW
all pressures ± .1"Hg. or H_2O

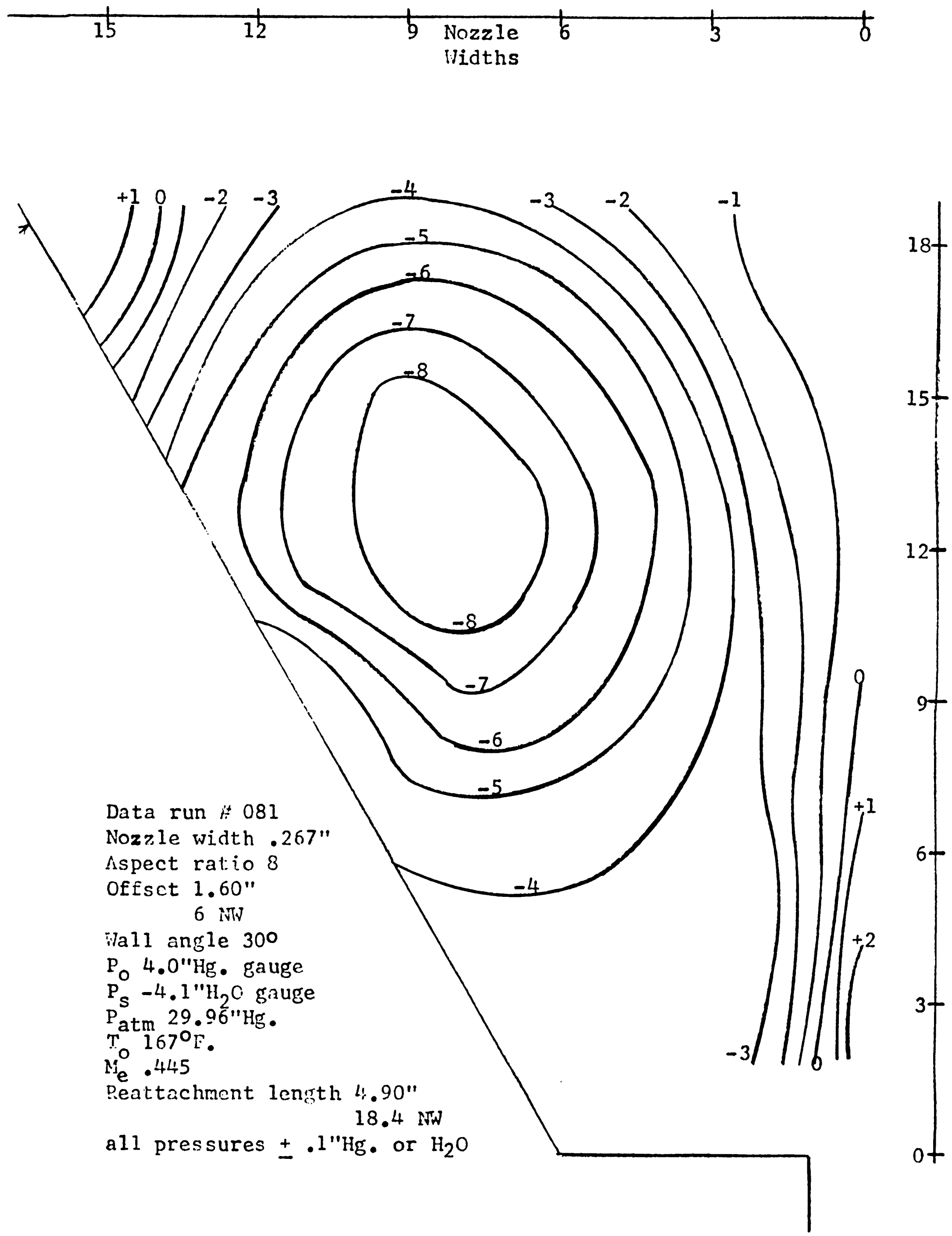

15
12
9
Nozzle Widths
6
3
0
+1
0
-2
-3
-4
-5
-6
-7
-8
-3
-2
-1
18
15
12
9
6
3
0
-8
-7
-6
-5
-4
0
+1
+2
-3
0
Data run # 081
Nozzle width .267"
Aspect ratio 8
Offset 1.60"
6 NW
Wall angle 30°
P_o 4.0"Hg. gauge
P_s -4.1"H_2O gauge
P_{atm} 29.96"Hg.
T_o 167°F.
M_e .445
Reattachment length 4.90"
18.4 NW
all pressures ± .1"Hg. or H_2O

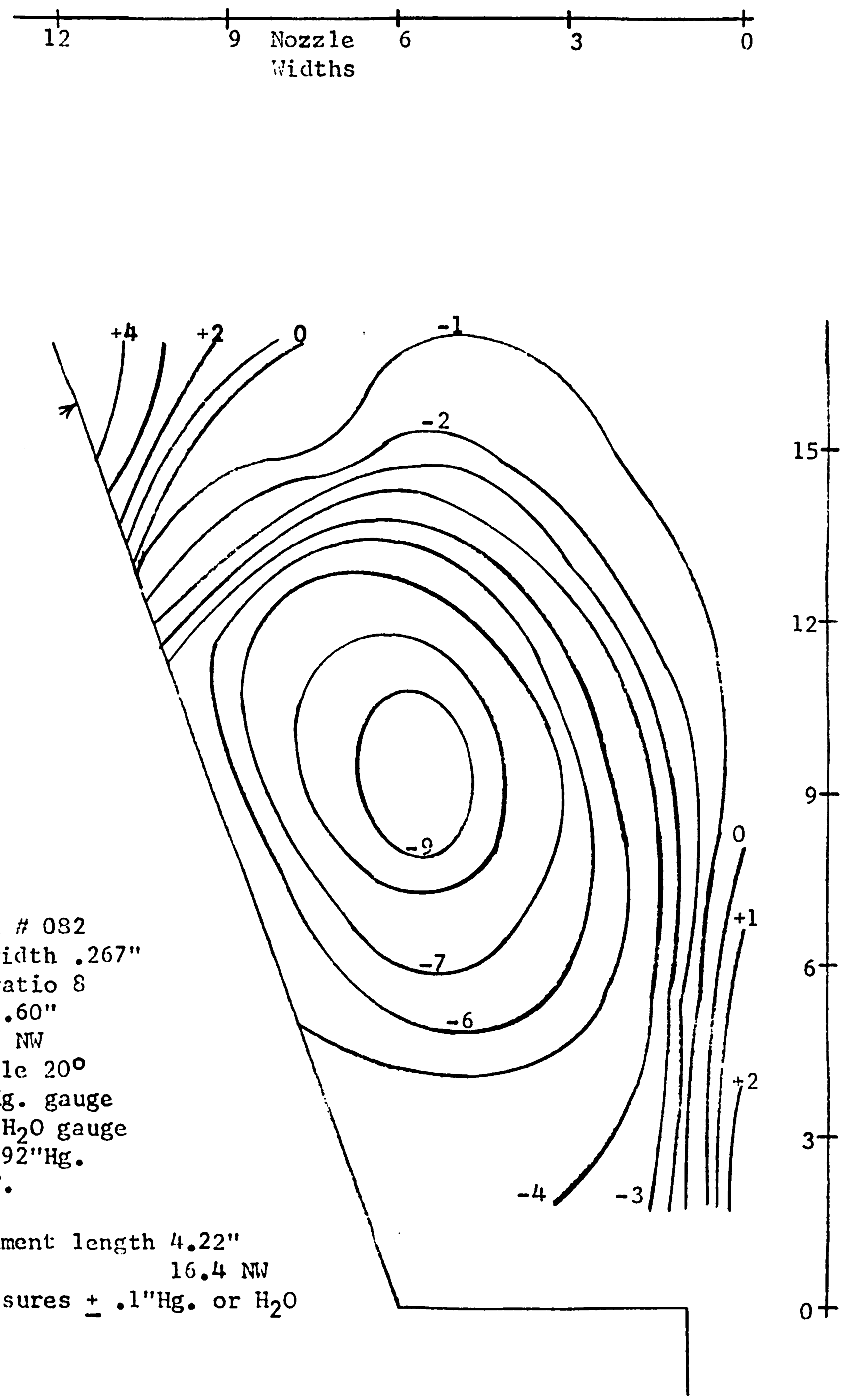

Data run # 082
Nozzle width .267"
Aspect ratio 8
Offset 1.60"
6 NW
Wall angle 20°
P_o 4.1"Hg. gauge
P_s -3.8"H_2O gauge
P_{atm} 29.92"Hg.
T_o 170°F.
M_e .448
Reattachment length 4.22"
16.4 NW
all pressures ± .1"Hg. or H_2O

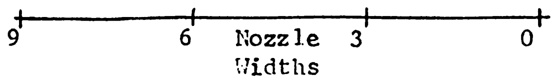

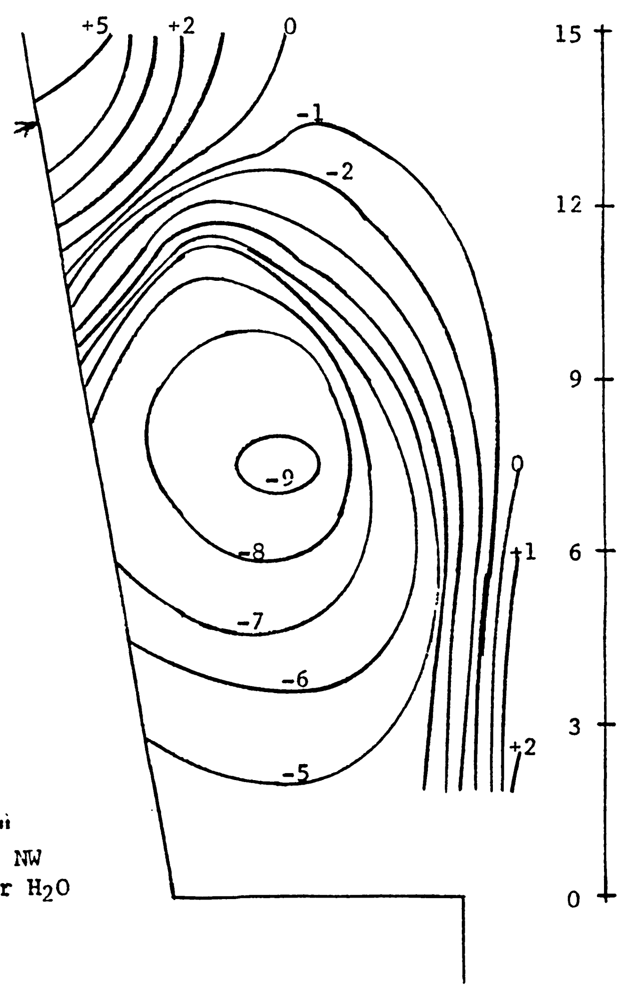

Data run # 091
Nozzle width .267"
Aspect ratio 8
Offset 1.60"
6 NW
Wall angle 10^{o}
P_o 4.1"Hg. gauge
P_s -4.2 "H_2O gauge
P_{atm} 29.95"Hg.
T_o 166°F.
M_e .449
Reattachment length 3.69"
14.4 NW
all pressures $\pm$ .1"Hg. or H_2O

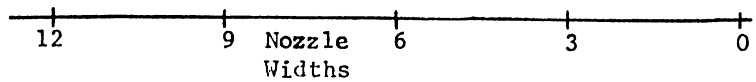

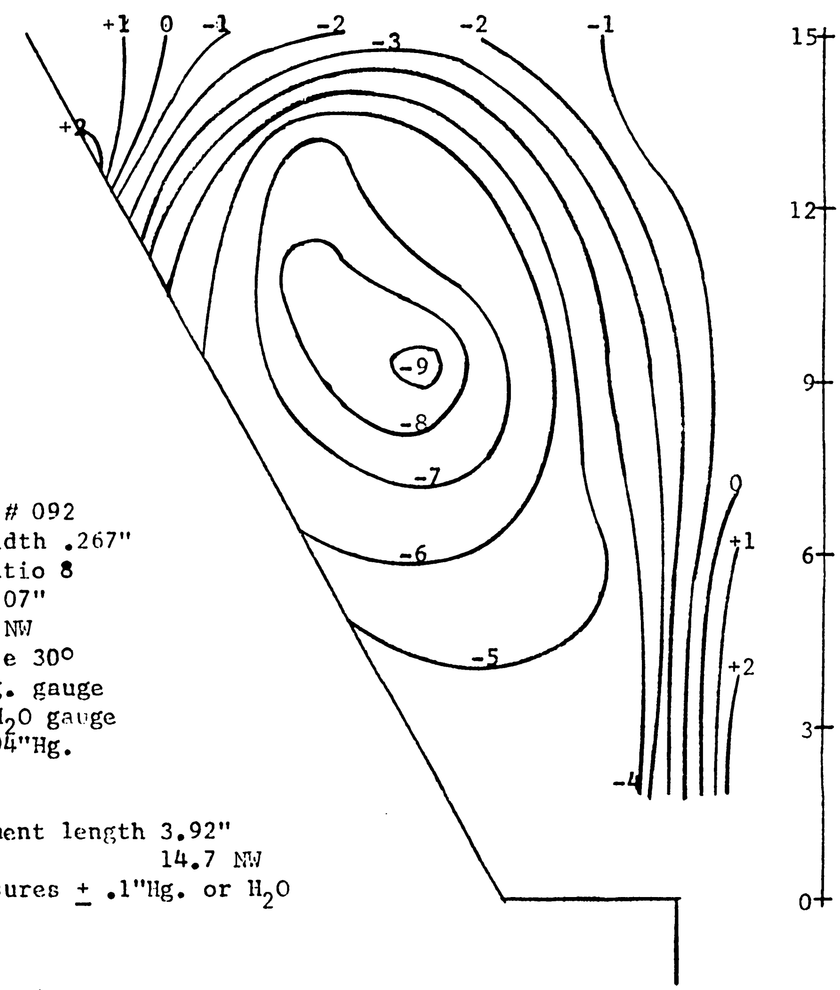

Data run # 092
Nozzle width .267"
Aspect ratio 8
Offset 1.07"
4 NW
Wall angle 30°
P_o 4.0"Hg. gauge
P_s -4.6"H_2O gauge
P_{atm} 29.94"Hg.
T_o 172°F.
M_e .447
Reattachment length 3.92"
14.7 NW
all pressures ± .1"Hg. or H_2O

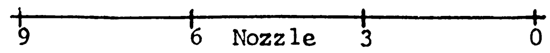

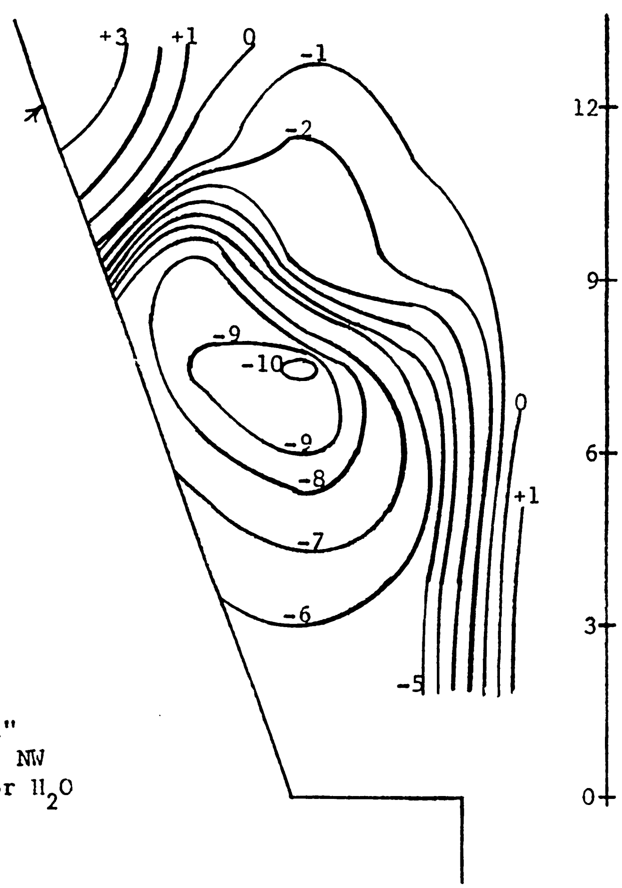

Data run # 093
Nozzle width .267"
Aspect ratio 8
Offset 1.07"
4 NW
Wall angle 20°
P_o 4.0"Hg. gauge
P_s -4.7"H_2O gauge
P_{atm} 29.89"Hg.
T_o 176°F.
M_e .450
Reattachment length 3.22"
12.1 NW
all pressures ± .1"Hg. or H_2O

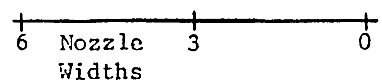

Data run # 101
Nozzle width .267"
Aspect ratio 8
Offset 1.07"
4 NW
Wall angle 10°
P_o 4.1"Hg.
P_s -5.6"H_2O
P_{atm} 29.96"Hg.
T_o 164°F.
M_e .454
Reattachment length 2.93"
11.0 NW
all pressures ± .1"Hg. or H_2O

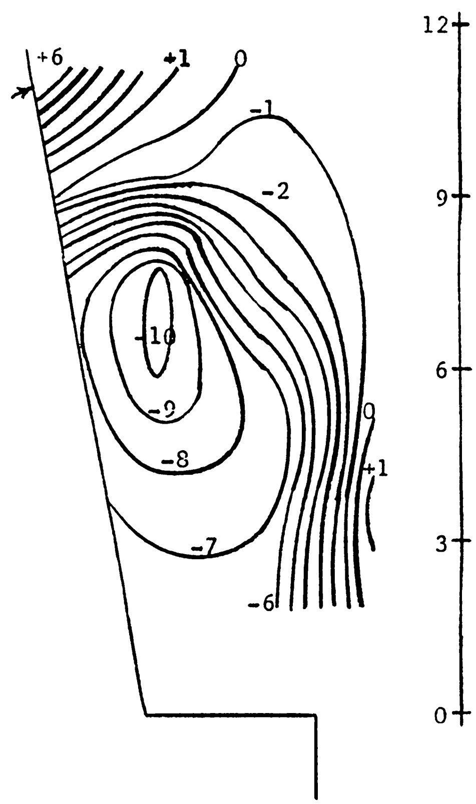

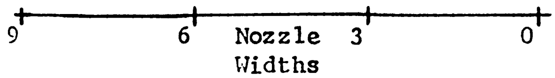

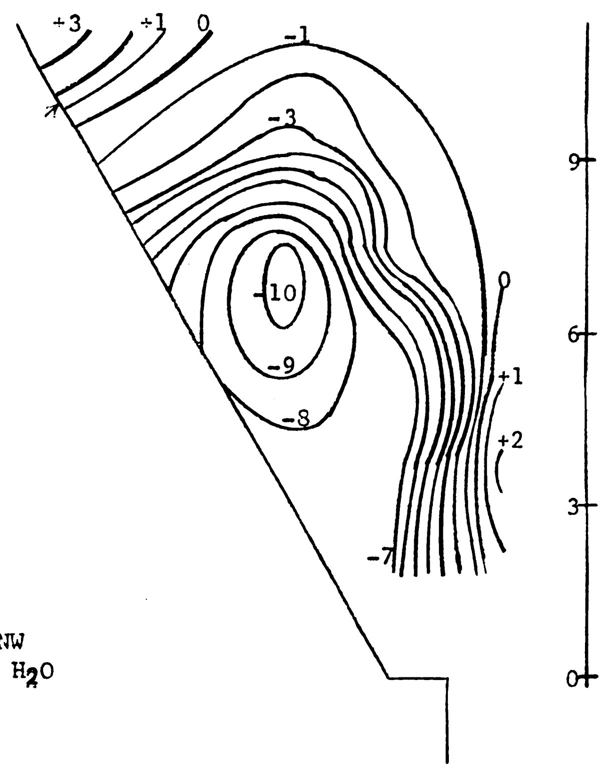

Data run # 102
Nozzle width .267"
Aspect ratio 8
Offset .53"
2 NW
Wall angle 30°
P_o 4.0"Hg. gauge
P_s -5.8"H_2O gauge
P_{atm} 29.97"Hg.
T_o 166°F.
M_e .453
Reattachment length 2.68"
10.0 NW
all pressures ± .1"Hg. or H_2O

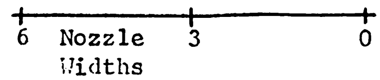

Data run # 103
Nozzle width .267"
Aspect ratio 8
Offset .53"
2 NW
Wall angle 20°
P_o 4.0"Hg. gauge
P_s -6.8"H_2O gauge
P_{atm} 29.93"Hg.
T_o 172°F.
M_e .457
Reattachment length 2.21"
8.3 NW
all pressures ± .1"Hg. or H_2O

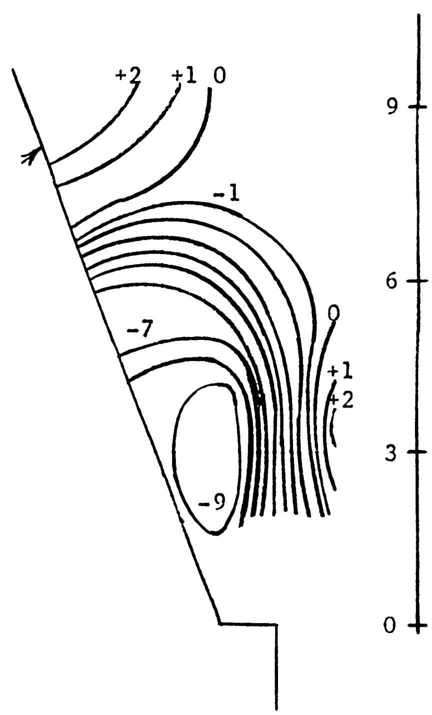

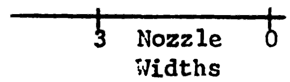

Data run # 104
Nozzle width .267"
Aspect ratio 8
Offset .53"
2 NW
Wall angle 10°
P_o 4.0"Hg. gauge
P_s -8.2"H_2O gauge
P_{atm} 29.89"Hg.
T_o 176°F.
M_e .461
Reattachment length 1.90"
7.1 NW
all pressures ± .1"Hg. or H_2O

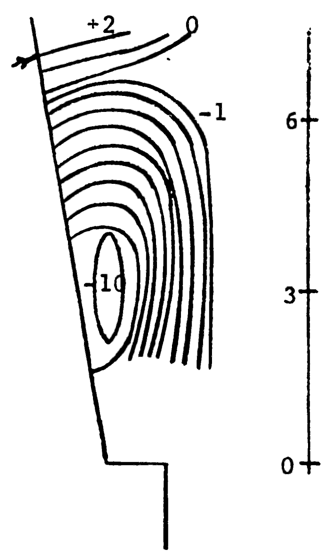

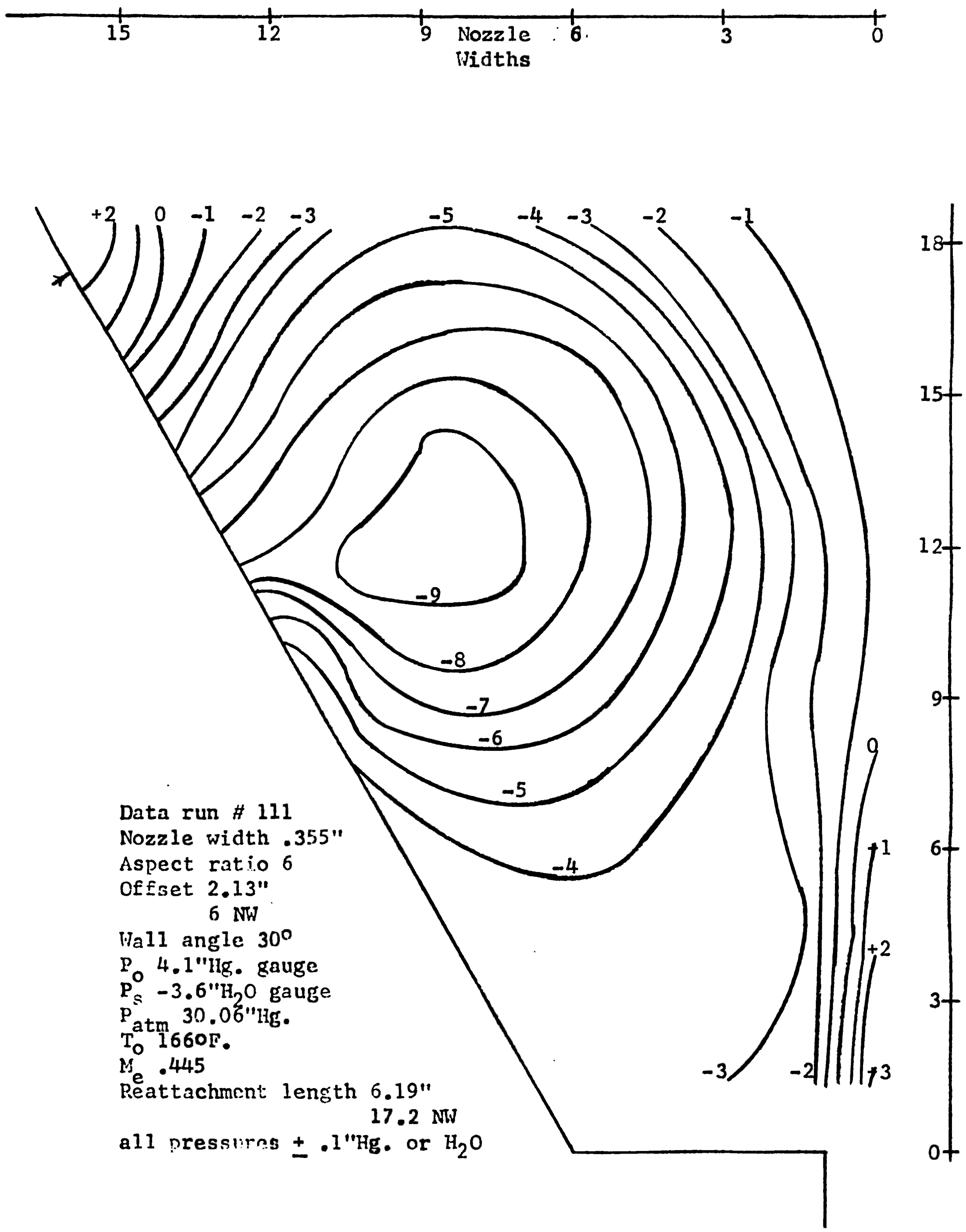
15
12
9
Nozzle Widths
6
3
0
+2
0
-1
-2
-3
-5
-4
-3
-2
-1
-9
-8
-7
-6
-5
-4
0
+1
+2
+3
-3
-2
18
15
12
9
6
3
0
Data run # 111
Nozzle width .355"
Aspect ratio 6
Offset 2.13"
6 NW
Wall angle 30°
P_o 4.1"Hg. gauge
P_s -3.6"H_2O gauge
P_{atm} 30.06"Hg.
T_o 166°F.
M_e .445
Reattachment length 6.19"
17.2 NW
all pressures ± .1"Hg. or H_2O

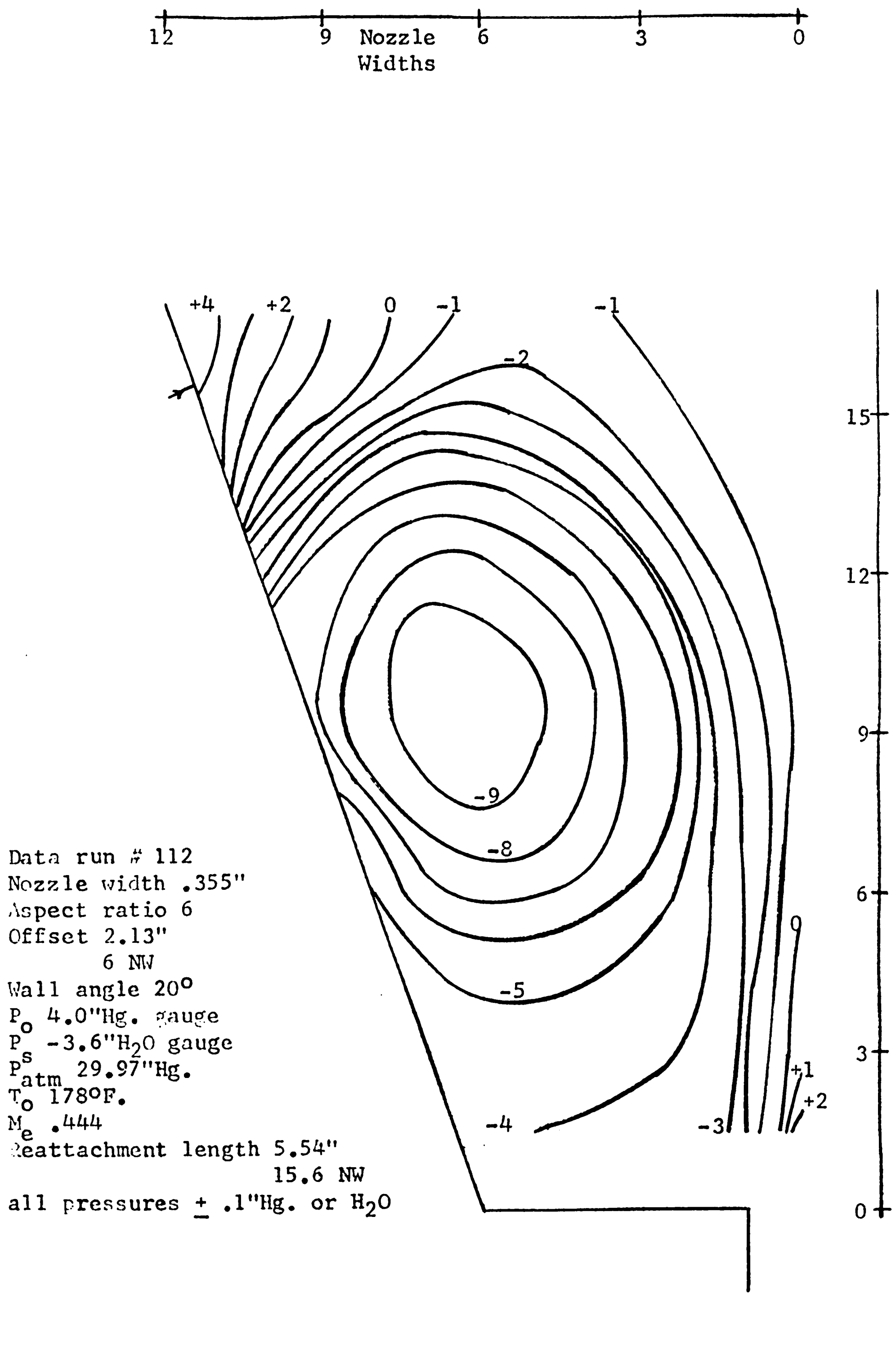

12
9
Nozzle Widths
6
3
0
+4
+2
0
-1
-1
-2
-9
-8
-5
-4
-3
0
+1
+2
15
12
9
6
3
0
Data run # 112
Nozzle width .355"
Aspect ratio 6
Offset 2.13"
6 NW
Wall angle 20°
P_o 4.0"Hg. gauge
P_s -3.6"H_2O gauge
P_{atm} 29.97"Hg.
T_o 178°F.
M_e .444
Reattachment length 5.54"
15.6 NW
all pressures ± .1"Hg. or H_2O

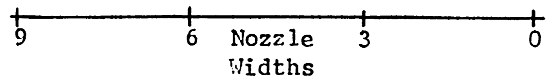

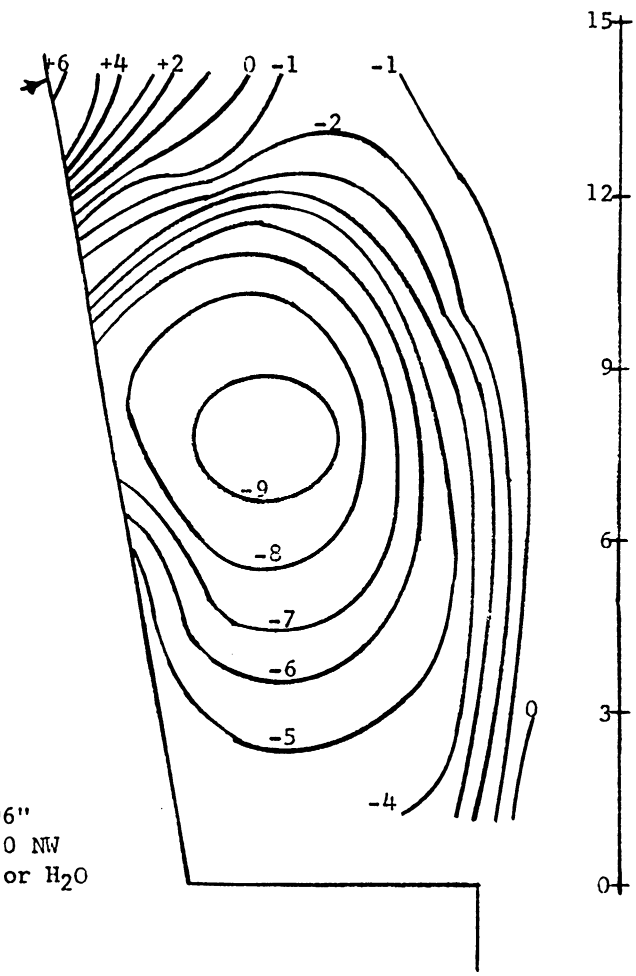

Data run # 121
Nozzle width .355"
Aspect ratio 6
Offset 2.13"
6 NW
Wall angle 10^{o}
P_o 4.0"Hg. gauge
P_s -3.8"H_2O gauge
P_{atm} 30.11
T_o 170^{o}F.
M_e .442
Reattachment length 4.96"
14.0 NW
All pressures ± .1"Hg. or H_2O

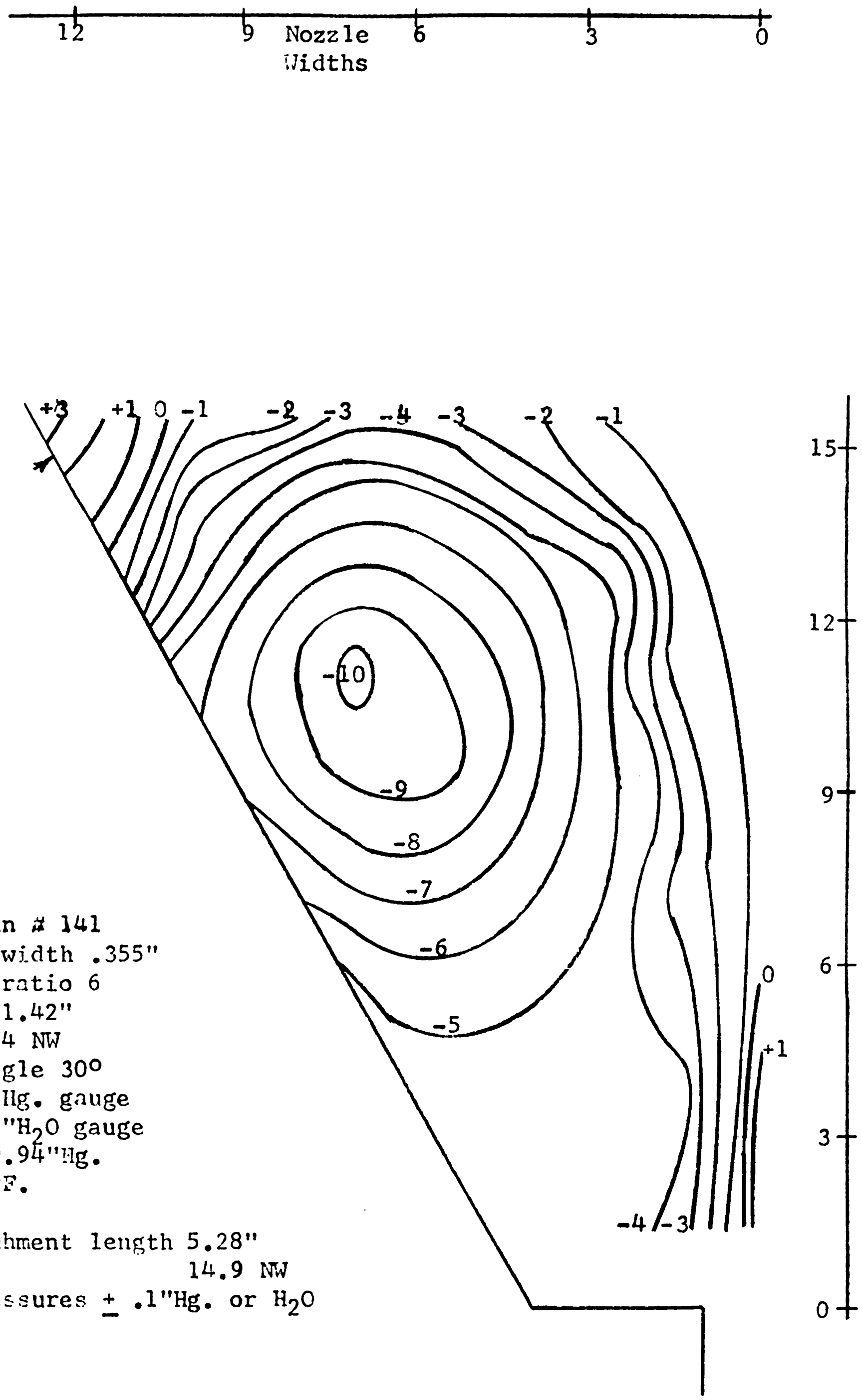

Data run # 141
Nozzle width .355"
Aspect ratio 6
Offset 1.42"
4 NW
Wall angle 30°
P_o 4.0"Hg. gauge
P_s -4.2"H_2O gauge
P_{atm} 29.94"Hg.
T_o 176°F.
M_e .447
Reattachment length 5.28"
14.9 NW
all pressures ± .1"Hg. or H_2O

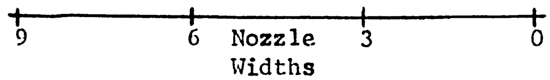

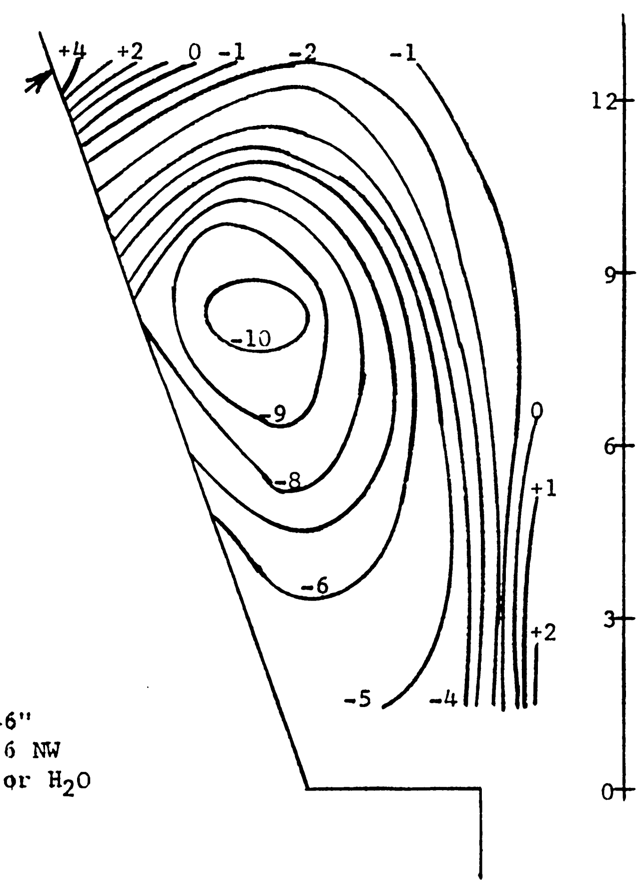

Data run # 151
Nozzle width .355"
Aspect ratio 6
Offset 1.42"
4 NW
Wall angle 20°
P_o 4.0"Hg. gauge
P_s -4.6"H_2O gauge
P_{atm} 29.94"Hg.
T_o 173°F.
M_e .447
Reattachment length 4.46"
12.6 NW
all pressures ± .1"Hg. or H_2O

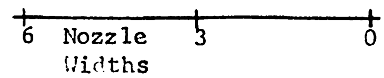

Data run # 152
Nozzle width .355"
Aspect ratio 6
Offset 1.42"
4 NW
Wall angle 10^{o}
P_o 4.0"Hg. gauge
P_s -4.6"H_2O gauge
P_{atm} 29.92"Hg.
T_o 177^{o}F.
M_e .448
Reattachment length 3.92"
11.0 NW
all pressures $\pm$ .1"Hg. or H_2O

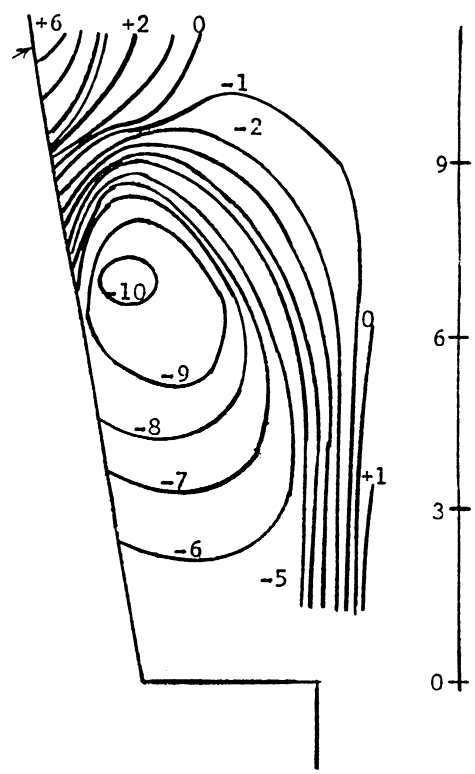

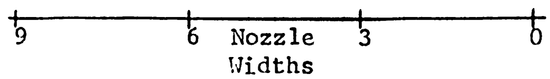

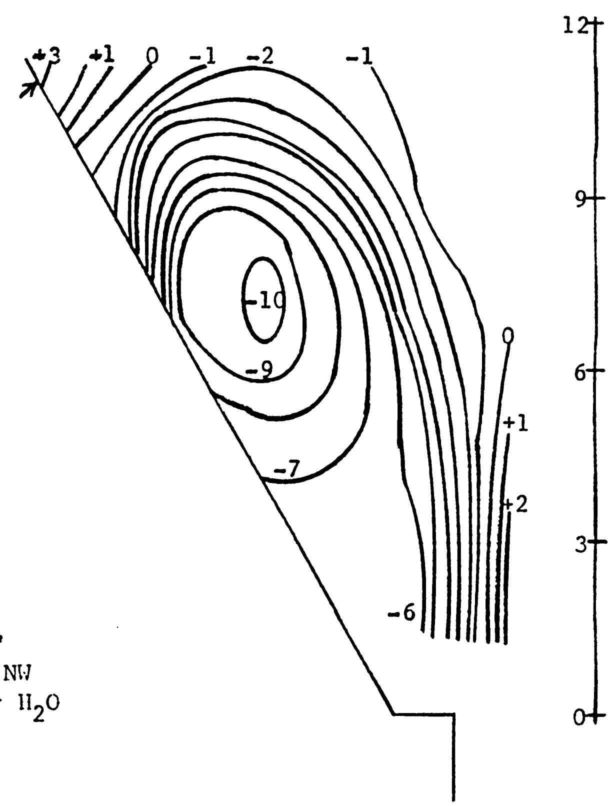

Data run # 161
Nozzle width .355"
Aspect ratio 6
Offset .71"
2 NW
Wall angle 30°
P_o 4.0"Hg. gauge
P_s -5.3"H_2O gauge
P_{atm} 29.99"Hg.
T_o 176°F.
M_e .449
Reattachment length 3.91"
11.0 NW
all pressures ± .1"Hg. or H_2O

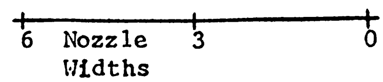

Data run # 162
Nozzle width .355"
Aspect ratio 6
Offset .71"
2 NW
Wall angle 20°
P_o 4.0"Hg. gauge
P_s -6.2"H_2O gauge
P_{atm} 29.98" Hg.
T_o 176°F.
M_e .454
Reattachment length 3.05"
8.6 NW
all pressures ± .1"Hg. or H_2O

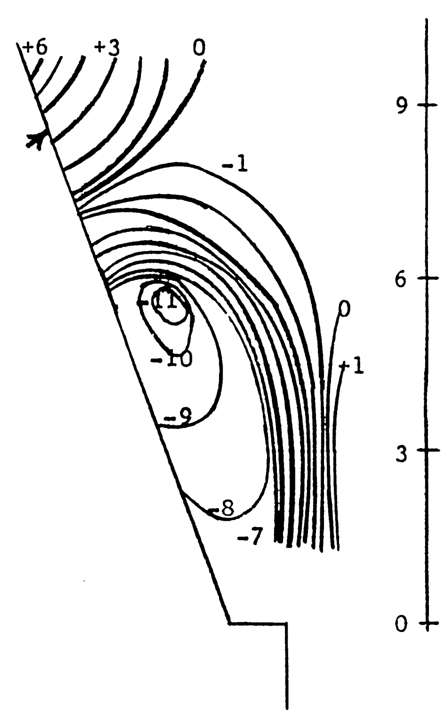

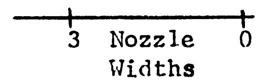

Data run # 163
Nozzle width .355"
Aspect ratio 6
Offset .71"
2 NW
Wall angle 10°
P_o 4.0"Hg. gauge
P_s -7.2"H_2O gauge
P_{atm} 29.97"Hg.
T_o 172°F.
M_e .458
Reattachment length 2.51"
7.1 NW
all pressures ± .1"Hg. or H_2O

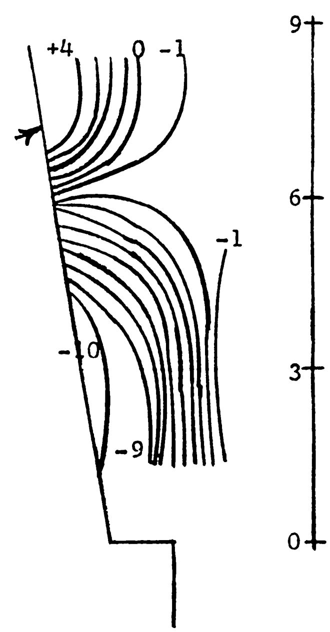

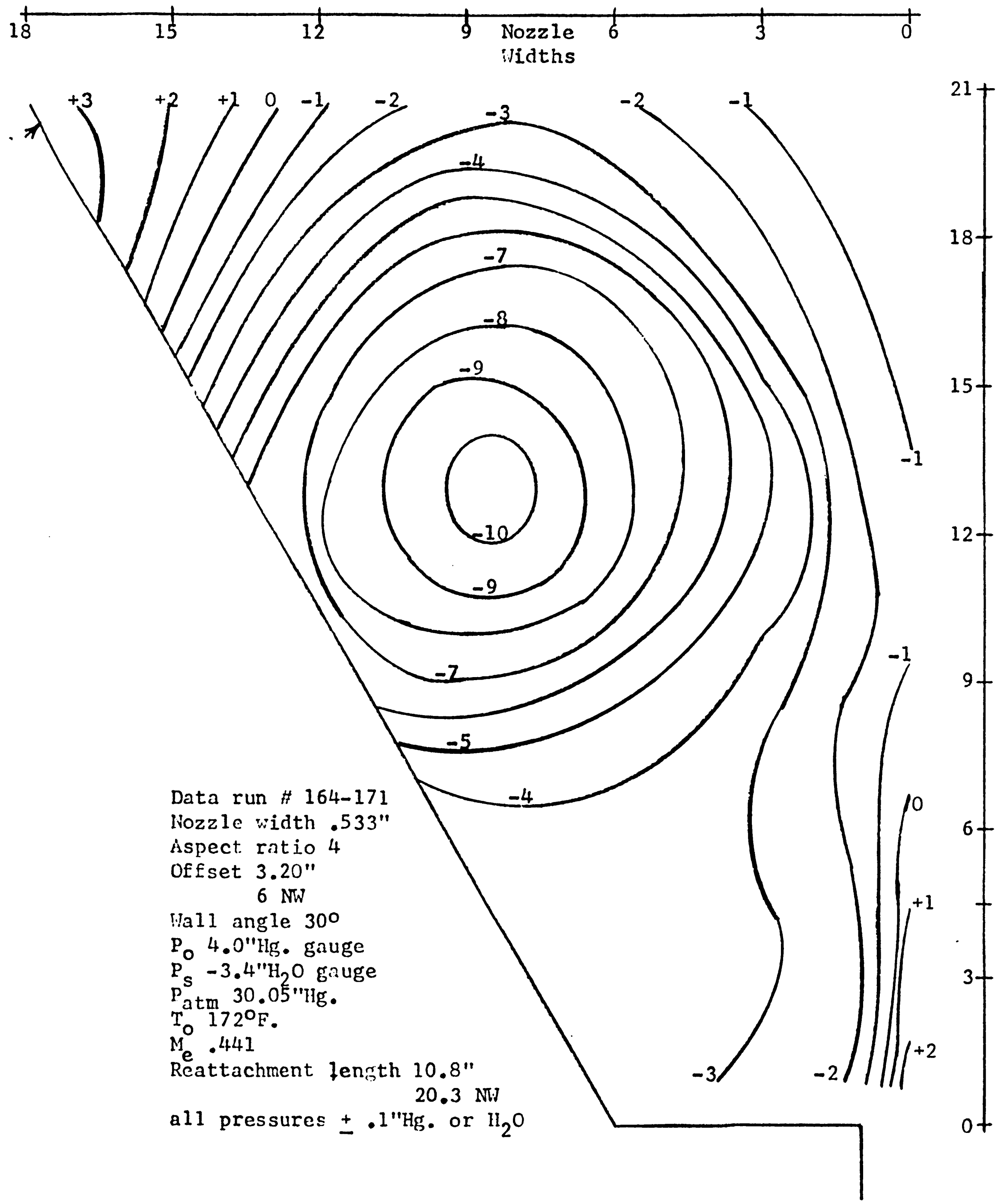
18
15
12
9
Nozzle Widths
6
3
0
21
18
15
12
9
6
3
0
+3
+2
+1
0
-1
-2
-3
-4
-7
-8
-9
-10
-9
-7
-5
-4
-2
-1
-1
-1
0
+1
+2
-3
-2
Data run # 164-171
Nozzle width .533"
Aspect ratio 4
Offset 3.20"
6 NW
Wall angle 30°
P_o 4.0"Hg. gauge
P_s -3.4"H_2O gauge
P_{atm} 30.05"Hg.
T_o 172°F.
M_e .441
Reattachment length 10.8"
20.3 NW
all pressures ± .1"Hg. or H_2O

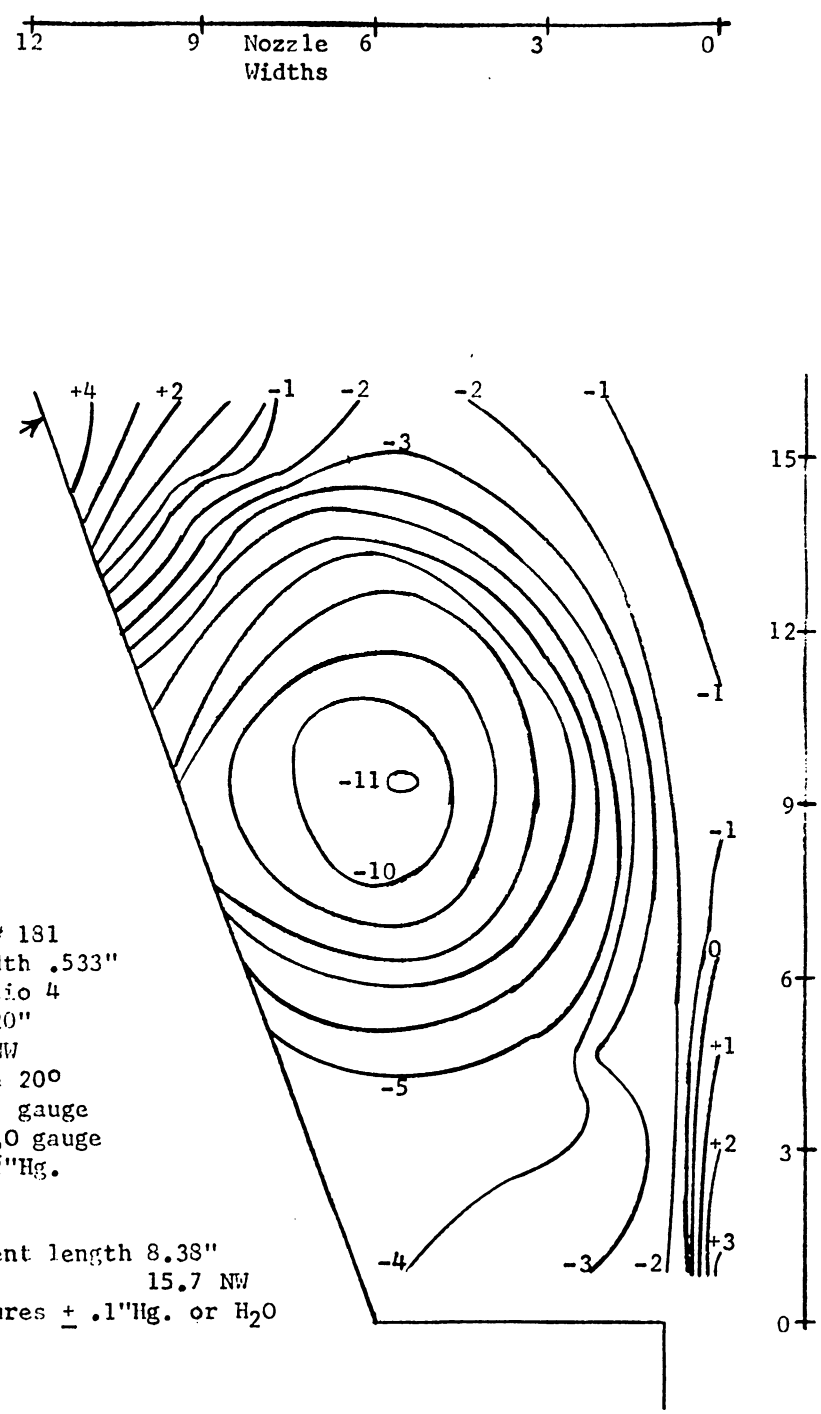

Data run # 181
Nozzle width .533"
Aspect ratio 4
Offset 3.20"
6 NW
Wall angle 20°
P_o 4.0"Hg. gauge
P_s -3.0"H_2O gauge
P_{atm} 30.12"Hg.
T_o 170°F.
M_e .439
Reattachment length 8.38"
15.7 NW
all pressures ± .1"Hg. or H_2O

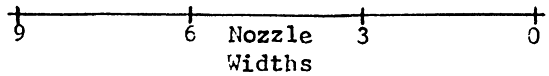

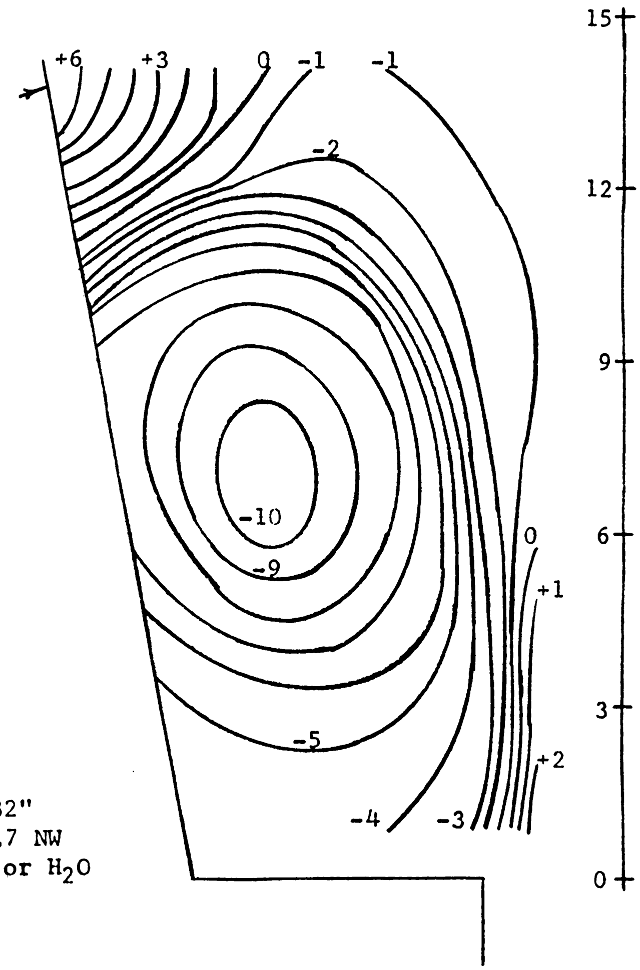

Data run # 191
Nozzle width .533"
Aspect ratio 4
Offset 3.20"
6 NW
Wall angle 10°
P_o 4.0"Hg. gauge
P_s -1.8"H_2O gauge
P_{atm} 29.96"Hg.
T_o 171°F.
M_e .434
Reattachment length 7.32"
13.7 NW
all pressures ± .1"Hg. or H_2O

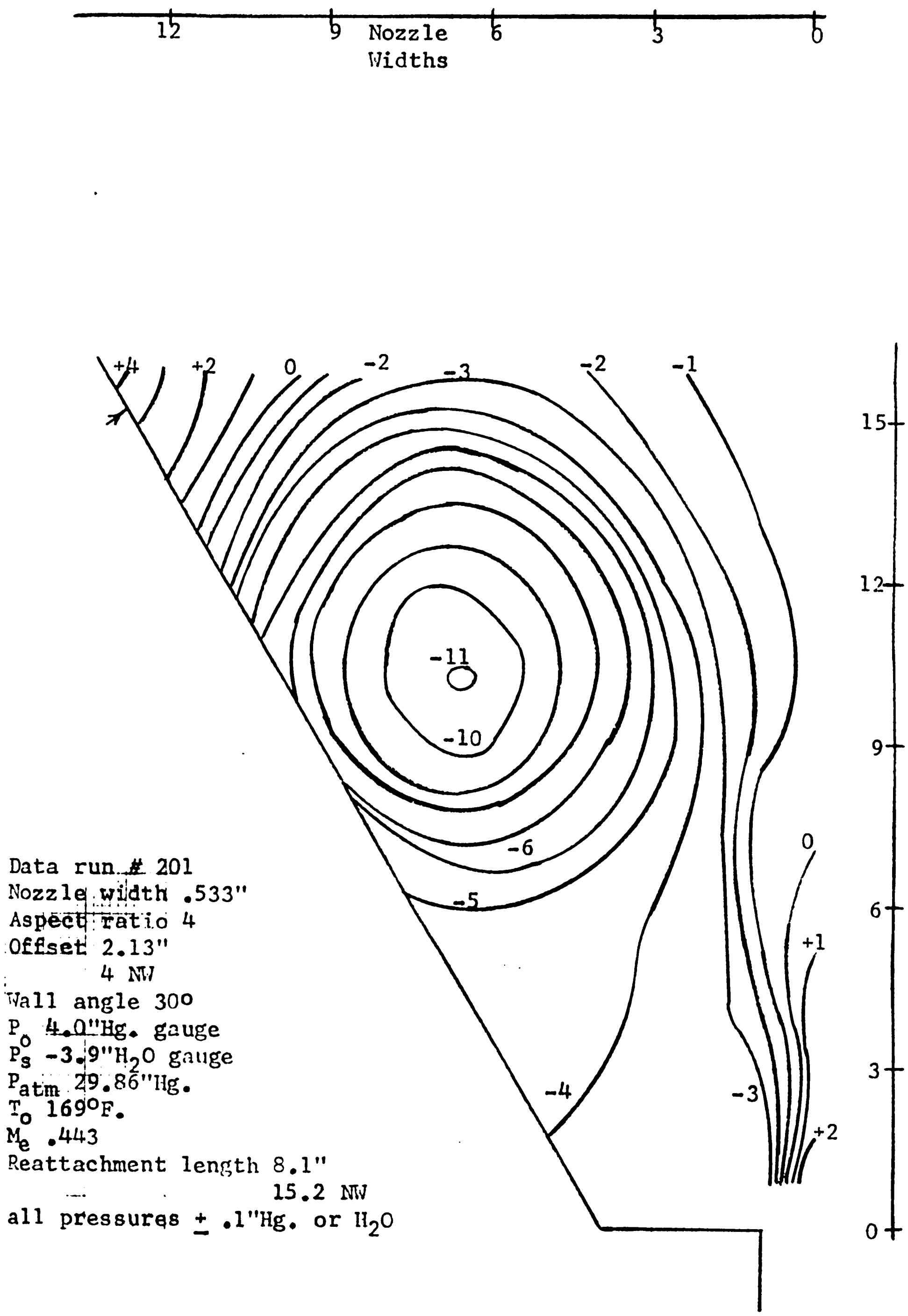

12
9
Nozzle
Widths
6
3
0
+4
+2
0
-2
-3
-2
-1
-11
-10
-6
-5
-4
-3
0
+1
+2
15
12
9
6
3
0
Data run # 201
Nozzle width .533"
Aspect ratio 4
Offset 2.13"
4 NW
Wall angle 30°
P_o 4.0"Hg. gauge
P_s -3.9"H_2O gauge
P_{atm} 29.86"Hg.
T_o 169°F.
M_e .443
Reattachment length 8.1"
15.2 NW
all pressures ± .1"Hg. or H_2O

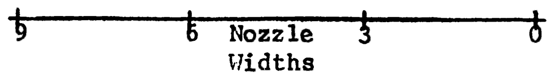

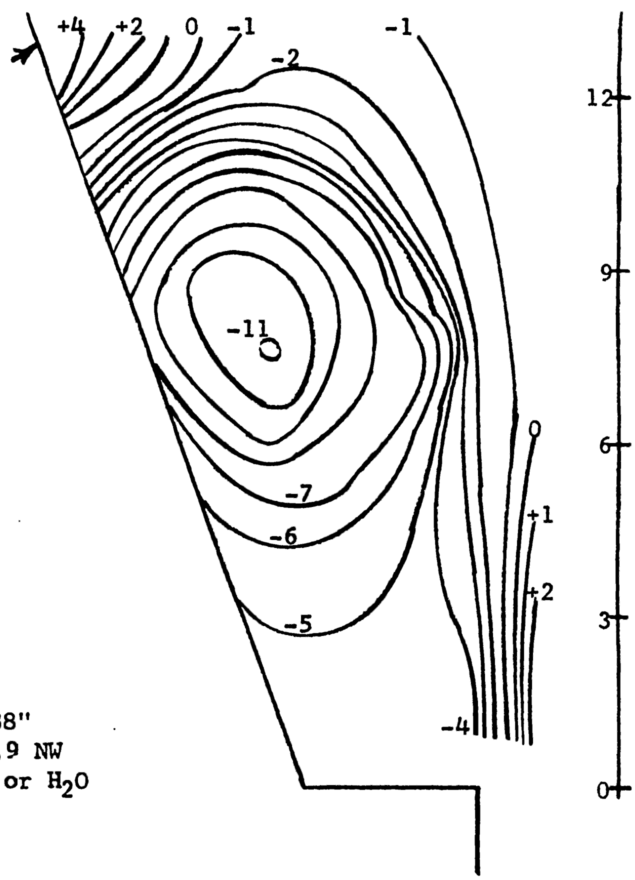

Data run # 211
Nozzle width .533
Aspect ratio 4
Offset 2.13"
4 NW
Wall angle 20°
P_o 4.0"Hg. gauge
P_s -4.2"H_2O gauge
P_{atm} 29.83"Hg.
T_o 170°F.
M_e .445
Reattachment length 6.88"
12.9 NW
all pressures ± .1"Hg. or H_2O

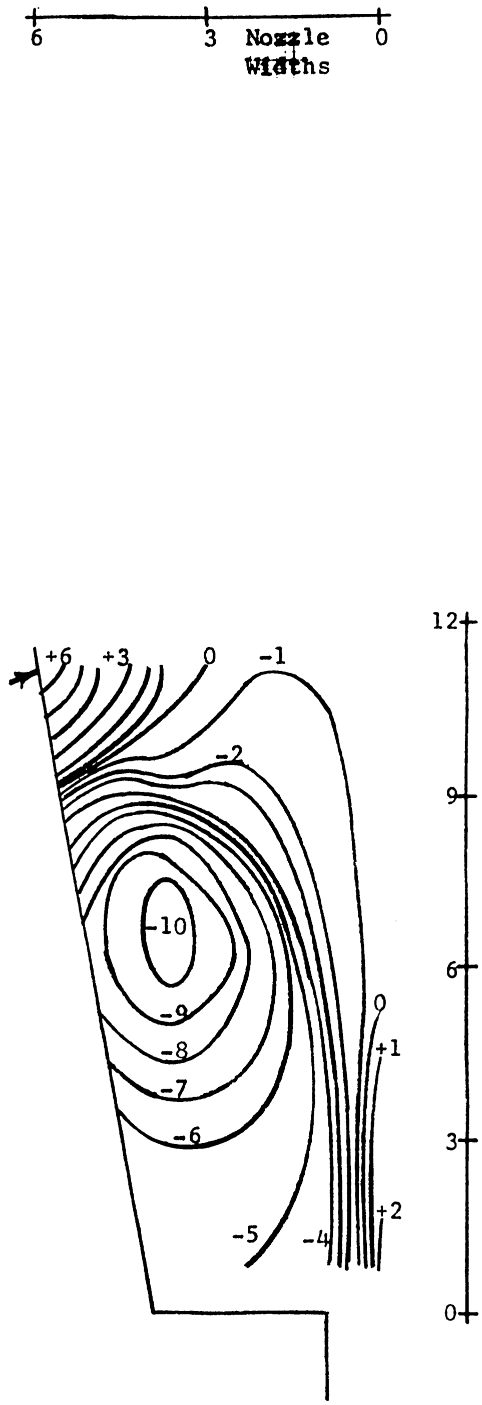

Data run # 221
Nozzle width .533"
Aspect ratio 4
Offset 2.13"
4 NW
Wall angle 10°
P_o 4.0" Hg, gauge
P_s -4.5"H_2O gauge
P_{atm} 29.89"Hg.
T_o 170°F
M_e .444
Reattachment length 5.94"
11.1 NW
all pressures ± .1"Hg. or H_2O

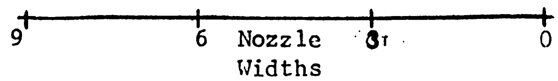

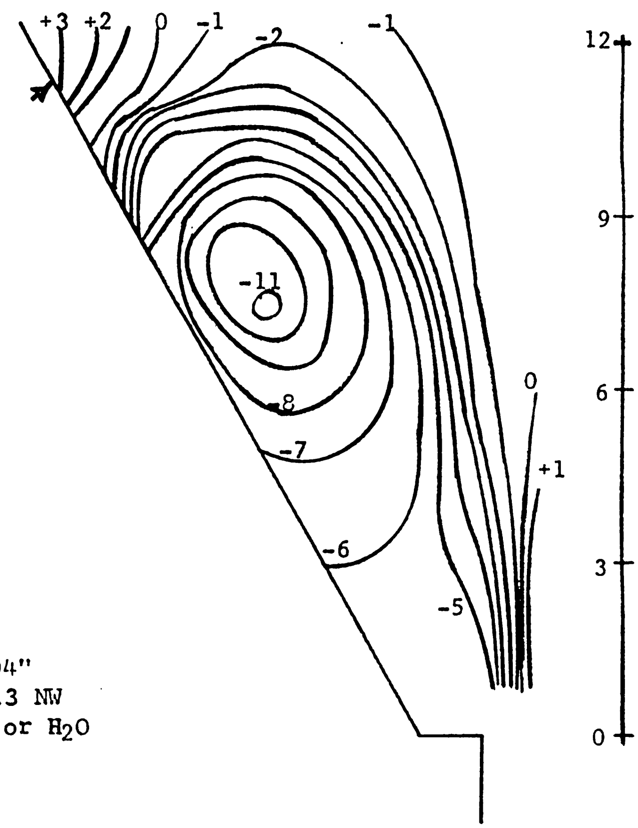

Data run # 222
Nozzle width .533"
Aspect ratio 4
Offset 1.07"
2 NW
Wall angle 30°
P_o 4.0"Hg. gauge
P_s -5.0"H_2O gauge
P_{atm} 29.88"Hg.
T_o 168°F.
M_e .446
Reattachment length 6.04"
11.3 NW
all pressures ± .1"Hg. or H_2O

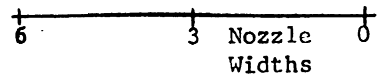

Data run # 231
Nozzle width .533"
Aspect ratio 4
Offset 1.07"
2 NW
Wall angle 20°
P_o 4.0"Hg. gauge
P_s -5.9"H_2O gauge
P_{atm} 29.96"Hg.
T_o 166°F.
M_e .450
Reattachment length 4.63"
8.7 NW
all pressures ± .1"Hg. or H_2O

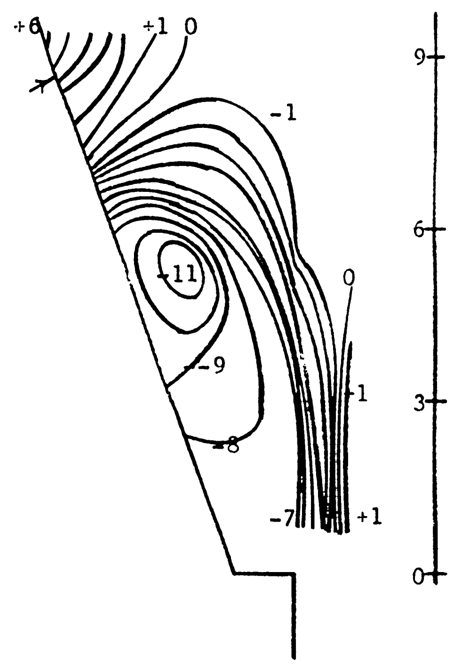

3 Nozzle 0
Widths

Data run # 232
Nozzle width .533"
Aspect ratio 4
Offset 1.07"
2 NW
Wall angle 10°
P_o 3.9"Hg. gauge
P_s -6.4"H_2O gauge
P_{atm} 29.97"Hg.
T_o 164°F.
M_e .449
Reattachment length 3.84"
7.2 NW
all pressures ± .1"Hg. or H_2O